USING LANDLAB, A FINE SCALE BIOGEOGRAPHY MODEL, TO MEASURE THE SUSTAINABILITY OF SEMI-ARID VEGETATION IN A CHANGING CLIMATE

By

Lucy Gelb

A thesis

Submitted in partial fulfilment

Of the requirements of the degree of

Master of Science in Hydrologic Sciences

Boise State University

May 2018

BOISE STATE UNIVERSITY GRADUATE COLLEGE

DEFENSE COMMITTEE AND FINAL READING APPROVALS

of the thesis submitted by

Lucy Gelb

Thesis Title: Using Landlab, a Fine Scale Biogeography Model, to Measure the Sustainability of Semi-Arid Vegetation in a Changing Climate

Date of Final Oral Examination: 2 November 2016

The following individuals read and discussed the thesis submitted by student Lucy Gelb, and they evaluated her presentation and response to questions during the final oral examination. They found that the student passed the final oral examination.

Alejandro N. Flores, Ph.D.	Chair, Supervisory Committee
Elowyn Yager, Ph.D.	Member, Supervisory Committee
Jennifer Pierce, Ph.D.	Member, Supervisory Committee
Nancy Glenn, Ph.D.	Member, Supervisory Committee

The final reading approval of the thesis was granted by Alejandro N. Flores, Ph.D., Chair of the Supervisory Committee. The thesis was approved by the Graduate College

ACKNOWLEDGEMENTS

This study was conducted in collaboration and cooperation with the United States Department of Agriculture Agricultural Research Service (ARS) Northwest Watershed Research Center (NWRC), Boise, Idaho and landowners within the Reynold Creek Critical Zone Observatory. This research was supported by National Science Foundation awards EAR-1331872 and IIA-1329513.

Thank you to Boise State University Geoscience Department and EPSCOR for the access to TREX, their Microsoft Windows Server 2012 providing Remote Desktop Services.

Thank you Sai Siddhartha Nudurupati for all your help with coding Landlab. I would also like to thank Katelyn FitzGerald, Jason Watt, and Miguel Aguayo for technical support, as well as Pam Aishlin for the meteorological data from Dry Creek Experimental watershed.

ABSTRACT

The distribution of vegetation in water-limited ecosystems is a product of complex and nonlinear interactions between climatic forcings (e.g., precipitation, temperature, solar radiation) and the underlying geomorphic template, which includes topography, geology, and soils. Changes in climate, particularly in precipitation and temperature, can dramatically alter the organization of vegetation. This is especially true in ecotones such as our area of study: the semi-arid transition between Great Basin shrub-steppe ecosystems and the coniferous forests of the Northern Rockies. Understanding and predicting how the spatial composition of terrestrial vegetation communities will change in these ecosystems is critical to predicting important future landscape changes such as landslides, erosion, fires, and water storage capacity. This study promotes understanding of the relative sensitivity of vegetation types to changes in weather and climate in water-limited environments using a land modeling framework. Specifically, we use the Landlab framework to develop and conduct a suite of numerical experiments that use ensemble methods to diagnose how changes in precipitation and temperature regimes affect the organization of plant functional types across varying hillslope aspects. This methodology yielded a broader perspective than previous studies that rely on analysis of deterministic runs, including detailed information about the variation within the results of each climate scenario we modeled. The impact of topographic variation such as changes in elevation or aspect are not not the same for temperature and precipitation, and understanding the

relative importance of each is useful when extending the implications of results from this study to varying real-world locations.

We synthesized a watershed using Landlab's landscape evolution capabilities to produce a topographic setting with contrasting hillslope aspects and randomly seeded vegetation (trees, shrubs, grasses, and bare soil). We then allowed that initial vegetation distribution to equilibrate to climatic conditions broadly consistent with contemporary climate. We then subjected the output distribution of vegetation to a perturbed climate, created by interpolating a group of Coupled Model Inter-Comparison Project 5 (CMIP5) climate projections that were downscaled using the Multivariate Adaptive Constructed Analogs (MACA) method to the approximate elevation of the site. We designed a suite of numerical experiments that investigated the sensitivity of the distribution of vegetation to changes in precipitation and temperature independently, as well as the combined effects of changes in both. To examine the sensitivity of vegetation composition to individual realizations of precipitation and temperature time series, and therefore the robustness of any conclusions about changes in vegetation composition to climate change, we took an ensemble approach with all simulations in which five-hundred realizations of precipitation and temperature forcings consistent with the altered climate were used to drive the climate change scenarios. We then investigated the probability density functions of the distribution of tree, shrub, grass, and bare soil coverage across aspects and simulations.

Regardless of scenario, we find that vegetation patterns on north-facing slopes were constant regardless of changes to precipitation or temperature alone. By contrast, vegetation patterns on south-facing slopes were sensitive to changes in both precipitation

and temperature. In climate scenarios with reduced precipitation, the percentage of area covered by trees declined on south-facing slopes, while shrub coverage increased to fill areas vacated by trees. Temperature exacerbated this trend. A climate scenario with low precipitation and high temperatures had the lowest recorded tree cover on south-facing slopes, though high precipitation negated the effects of temperature. Using the Landlab framework allowed us to rapidly develop an effective model of the relative sensitives of vegetation types and conclude that precipitation is the most important variable with regard to forest replacement by grasses and shrubs in response to climate change. It is important to underscore, however, that the modeling framework used does not currently include key biogeochemical processes known to influence semi-arid ecosystems. As such, this study cannot examine nutrient limitations in these semi-arid ecosystems. This suggests a potential avenue for future study that leverages the modeling framework and approach taken here.

TABLE OF CONTENTS

LIST OF TABLES

LIST OF FIGURES

INTRODUCTION

In arid, water limited ecosystems, changes in weather and climate have the potential to drastically alter the spatial organization of vegetation through interactions between climate, soils, and topography (Istanbulluoglu et al., 2008; Ivanov, Bras, & Vivoni, 2008; Vivoni et al., 2008; Yetemen , Istanbulluoglu, & Vivoni, 2010). Plant species modify their environment in varying ways. For example, they break down bedrock, facilitate the development of soil, and store and transpire water. Different plants have different impacts, and if plant distributions change, it is important that we anticipate that change to plan for, and predict ramifications to, changes in water storage capacity, ecosystem services, erosion, and natural disasters such as landslides and fires (Abrahams., Parsons, & Wainwright, 1995; Caylor, Manfreda, & Rodriguez-Iturbe, 2005; Collins & Bras, 2008; Istanbulluoglu et al., 2004; Malanson et al., 2007; Marston, 2010; Tucker & Bras, 1998). The need for this knowledge is especially urgent for arid and semi-arid environments, which cover about 45% of Earth's surface (Schimel, 2010) and are particularly susceptible to changes in precipitation and temperature (Ma et al., 2015). Previous work has researched the effects of drought and changes in temperature on ecosystems (W. R. L. Anderegg, Kane, & L. D. L. Anderegg, 2013; Bates et al., 2006; Schwinning, Starr, & Ehleringer, 2005a; Williams et al., 2012; Yetemen et al., 2015), but little work has been done to tease out which of the two is more important, although Grossiord et al. (2017) have researched this in a semi-arid woodland. The goal of our research is to promote fundamental understanding of the relative sensitivity of vegetation

types to changes in precipitation and temperature in these water-limited environments using a numerical modeling approach. Using locally sourced historical climate data and the modeling framework Landlab, we demonstrate the relative importance of changes in precipitation and temperature on the distribution of PFTs (Plant Functional Types) at the critical transition between a shrub-steppe and coniferous forest ecosystem.

Influences of Aspect on Vegetation

Vegetation growth is dependent on climate. The amount of precipitation or solar insolation an area receives will dictate what species of plants can grow there, as well as how healthy those individual plants will be. This climactic control on plant life can be explored on many levels; in water-limited environments, however, the most significant control on vegetation development and growth is the availability of water. Water availability is dependent on how much precipitation an area receives, and the amount of that precipitation that is retained within the landscape for a sufficient amount of time for local vegetation to utilize it. Precipitation can take the form of rain or snow. Rainwater that infiltrates into the soil is relatively rapidly accessible to plants through their roots. The ability of soil, therefore, to retain that water is also integral to the growth of vegetation (Rodriguez-Iturbe, 2000). Precipitation that falls as snow changes the timing of water availability. With rain, water is available almost instantly, while snow accumulates on the ground and is not accessible until it melts. Though precipitation phase significantly affects the timing and availability of plant available water, the current version of the developed model does not account for the accumulation and melt of a snowpack and treats all precipitation as rain.

The above assumes the plant is a mostly passive recipient of water, but that characterization does not paint a full picture: plants also modify their environment in ways that can change not only water storage, but also the climate itself. Vegetation breaks down bedrock with their roots, through both physical and chemical weathering mechanisms. Chemical weathering occurs when roots secrete weak acids that break up rocks on a molecular level, whereas physical weathering occurs when roots grow in ways that wedge rocks apart, forcing themselves into weaknesses in rock and driving cracks wider with their growth. Once bedrock is broken up, it can remain in place, potentially exposing more surfaces and fractures to chemical and physical weathering processes and eventually creating soil. Plant life, using their root systems as a matrix, holds soil and regolith in place and plant canopies intercept rainfall that may otherwise exert erosive forces on soils (Burroughs & Thomas, 1977; DeGraff, 1979; Kuruppuarachchi & Wyrwoll, 1992; O'Loughlin, 1974; Riestenberg & Sovonick-Dunford, 1983; Roering et al., 2003; Schmidt et al., 2001; Terwilliger & Waldron, 1991; Wu, McKinnell III, & Swanston, 1979). Increased precipitation and vegetation cover has been linked to steeper slopes (Collins & Bras, 2008; Jeffery et al., 2014). In this way, vegetation facilitates the development of soil and can further serve to resist erosive mechanisms, which has the effect of creating more space for water storage in the soil. Since (simplistically) water in excess of soil storage results in runoff, which exerts shear stress on the landscape and may enhance erosion, vegetation further serves to damper soil loss. In this way, plants participate in a positive feedback loop, developing an environment that is more hospitable to themselves so that more plants can grow in area.

Solar radiation also exerts significant control on the circulation of water in the hydrologic cycle because it dominates the energy available to drive evapotranspiration. Though the processes through which solar radiation changes local climate are complicated and interconnected, we focus here on a single term than encapsulates many related factors: potential evapotranspiration (PET). Evaporation is the process through which water changes from its liquid to a gaseous phase and evapotranspiration refers to the sum of evaporation from unvegetated surfaces and transpiration facilitated by plants, which respire water and oxygen into the air as they photosynthesize. PET is the maximum amount of water that the soil-vegetation system can transpire into the atmosphere over a given period and for defined climate conditions. This term is independent of actual water availability, instead expressing merely a hypothetical maximum atmospheric water demand given no constraints on water. Among other variables, air temperature, net irradiance, vapor pressure deficit, and individual plant species' characteristics all contribute to determining PET. These variables are all interconnected, and depend in various amounts on solar radiation received.

Solar radiation is affected by topography and position on the globe. Due to the curvature of the Earth, at the equator the Sun's radiation strikes the Earth's surface nearly perpendicularly, whereas at higher latitudes (both negative and positive), solar radiation approaches the earth at non-orthogonal angles. The lower solar angles with increasing latitude are associated with radiation being delivered over a larger area. These latitudinal effects are also modified by a hillslope. For example, in the northern hemisphere, the angle of a south-facing hillslope can mitigate the effect of being located at a higher latitude, creating a plane that is closer to perpendicular to the Sun's beams than a flat

surface is. By contrast, a north-facing hillslope at that same location would exacerbate the effects of latitude.

These aspect-driven differences in radiation can have profound effects on vegetation. Species distributions and plant health can change dramatically from one hillslope to the next, even within a relatively small geographic area. In the semi-arid ecosystems in our study area in the northern hemisphere (Dry Creek Experimental Watershed), this is often expressed with trees predominantly growing on north-facing hillslopes and species better adapted to lower water availability, such as shrubs or grasses, primarily growing on south-facing hillslopes. Over time, this difference in plant distribution creates changes on the hillslopes themselves. Trees with deep root systems tend to hold soil in place, supporting a deeper soil profile that is difficult to erode. Thus, on north-facing hillslopes in our area, slope angles tend to be more extreme than south-facing ones, exhibiting hillslope asymmetry (Tesfa et al., 2009). On south-facing aspects in this landscape, soil depths tend to be smaller than on north-facing slopes, although the precise mechanisms responsible for the coevolution of soils, hydrologic response, and plant community composition on these hillslopes remains unclear. What is evident, however, is that on south-facing soils in this landscape the soil tends to be more vulnerable to erosion. Variation in soil texture, not just quantity, is also associated with differences in local vegetation and climate (Geroy et al., 2011). Though these exact responses to hillslope aspect are not uniform (e.g. steep north-facing aspects with deep soils), even within the northern hemisphere, aspect-driven hillslope asymmetry is consistently present and has been thoroughly documented (Burnett, Meyer & McFadden, 2008; Istanbulluoglu et al., 2008; McAuliffe et al., 2014; Poulos et al., 2012).

In all the ways discussed in the proceeding paragraphs, the spatial distribution of vegetation plays an important role in the evolution of Earth's Critical Zone in water-limited systems. Though we know much about these connections, there remain significant uncertainties in the relative importance of water availability and temperature on the hillslope-scale distribution of vegetation types. Our research aims to investigate those connections further, using a suite of modeling experiments to modify and hold constant those variables as needed to compare their impacts on the geographic distribution of vegetation.

Modeling Background

Global biogeography models (GBMs), while useful for investigating vegetation trends on the scale of the world, represent areas too large to be useful in studying changes in PFTs across microclimates. Small changes in elevation or hillslope aspect can drastically alter the solar radiation and precipitation received at a given location and, particularly, in mountain landscapes these variables that exert physiographic control on vegetation distribution can change dramatically over small distances (C. Hanson & Johnson, 2001). These influences have a nonlinear effect on local vegetation (Manfreda & Caylor, 2013). Many different microclimates can exist within one valley, all supporting their own ecosystem and PFTs (Istanbulluoglu et al., 2008; Thompson, Katul, & Porporato, 2010). These climate variations are important when characterizing the larger landscape and maintaining species diversity (Caracciolo et al., 2014), but limits in computing power make them impossible to capture with GBMs.

Using Landlab (G. Tucker, 2013), we investigate how changes in microclimate perturb vegetation in semi-arid regions at the ecotone between shrublands and coniferous

forests. Landlab is a modern landscape modelling software framework that allows users to quickly develop sophisticated models that couple key Earth surface processes using a high-level scientific programming language, Python. Its modular nature allows users to easily develop and test complex models of coupled eco-geomorphic systems, allowing them to select relevant processes to include without the need to couple a variety of different models together (Hobley et al., 2017). Two important existing components within the Landlab framework include the dynamical plant modeling of CATGRASS (Zhou, Istanbulluoglu, & Vivoni, 2013) and landscape evolution functionality that is largely consistent with the Channel-Hillslope Integrated Landscape Development (CHILD) model (G. E. Tucker et al., 2001). CATGRASS uses cellular automata and hydrological constraints to model the distribution of PFT growth. CHILD uses a longer timescale to model the evolution of topography as forced by base-level change (e.g., tectonic uplift) and under the influence of erosive processes that include soil creep and stream power erosion. The Landlab modeling framework allows us to leverage the distinct capabilities of these models, without the significant software engineering challenges associated with coupling models of this nature.

To address the effects of terrain morphology on vegetation, prior studies have conducted simplistic global warming experiments that have added variation within a single model, such as a large elevation gradient that acts as a space-for-time substitution (Caracciolo et al., 2014). This strategy is useful when there are restrictions on computational power, but limits our ability to verify the statistical significance of model outcomes due to the limited data (a single deterministic output for each climate) that results from such an experiment. Our approach, instead, additionally considers

uncertainty associated with the internal variability in climate projection data to develop a more probabilistic depiction of likely transitions in hillslope-scale vegetation distributions, thereby adding robustness to our conclusions. We accomplish this by using climate projection data to obtain key parameters of a stochastic weather generator model and then performing many numerical experiments with realizations of weather that are stochastic but, taken together, consistent with the underlying climate projections. By running a plausible alternative climate scenario (i.e., a so-called "ensemble member") 500 times, we can characterize the distribution of results instead of a relying on a single model run and assuming it is a representative result.

While it is common for GBM models to use synthetic meteorological data, our research uses data from meteorological stations located within Dry Creek Experimental Watershed (DCEW), north of Boise, ID in the northwestern United States. DCEW spans a range of semi-arid ecosystems. The site within DCEW that we focus on in this study (named Treeline) receives about 650 mm of rain each year, with trees on north-facing slopes and shrubs and grasses on south-facing ones. Using historical meteorological data allows us to create realistic climate scenarios that are rooted in local measurements. To create our hypothetical climate scenarios, we used future projections from global climate models. These models had been downscaled with the MACA method (Abatzoglou & Brown, 2012) to create predictions that have been bias-corrected based on historical observations, and we further interpolate within them to obtain site-specific climate projections for our local study site in DCEW. These projections were then used to parameterize the stochastic weather generator and allowed us to model the vegetation in changed climates using climate forcings that are localized to not only a general semi-arid

ecosystem, but the exact watershed and elevation at which our study site is located. Our intent is to study microclimate, which can be highly variable within a single watershed.

METHODS

Site Location

Located in foothills to the northeast of Boise, ID, in the western United States (Figure 1, left), DCEW is 28 km2, and located on the divide between wet, forested mountains to the north and the dry, low-lying, Snake River Plain to the south. Due to its location along an ecotone, DCEW is a useful example of vegetation and weather patterns in a transition zone of a semi-arid ecosystem. Elevation and aspect directly control the vegetation present in this area (Anderson et al., 2014). Drought-tolerant sagebrush covers the lower parts of the watershed, while at higher elevations the land cover is a mix of Douglas Firs and Ponderosa Pines that require greater precipitation (Figure 2). Logging took place in the upper elevations throughout the last century (Loughridge, 2014), leaving legacy effects on the terrestrial ecosystem that are observed as locations that are missing trees in certain areas of the watershed that would otherwise be (and were historically) forested. The middle elevations exhibit a mix of the two ecosystems: south-facing hillslopes that receive more radiation grow shrubs and grasses while evergreens dominate north-facing aspects. Throughout the watershed, riparian species line the rivers, but we do not consider riparian species distributions owing to complexities in the presence and composition of riparian vegetation communities that cannot, at present, be captured by the Landlab framework. Distributed along this ecosystem gradient are a series of DCEW weather stations (McNamara, 1999). The focus of this study is the Treeline weather station, located at a middle elevation, on a ridge-line, and in the transition zone between

shrubs and trees (Figure 1, right). This weather station was the source of our historical data.

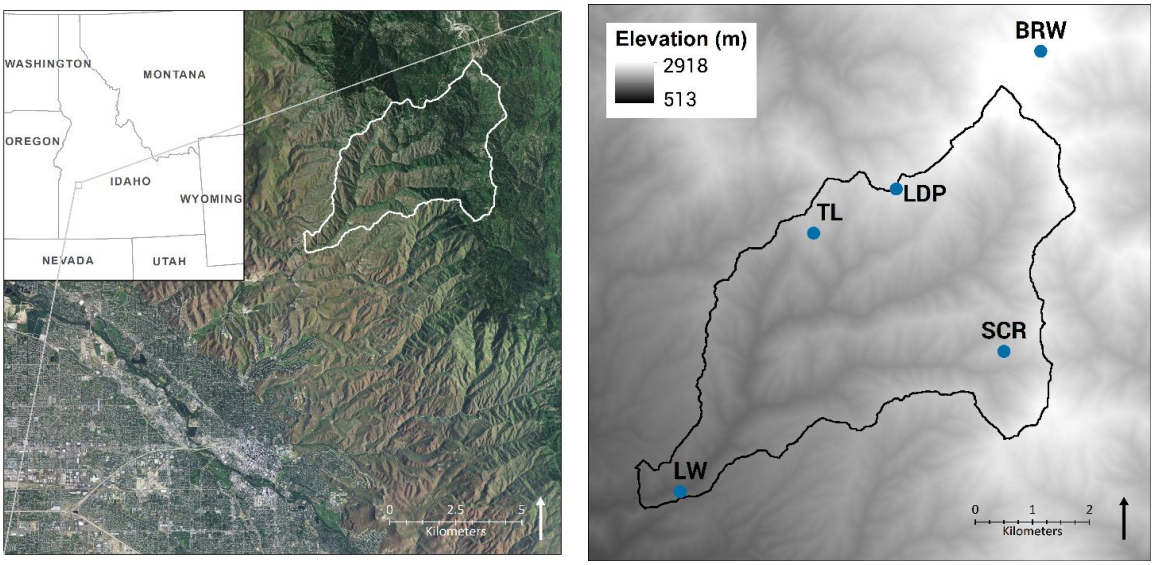

Figure 1: (left) Dry Creek Experimental Watershed (DCEW) is Located Northeast of Boise, ID. (right) Location of the Five Different Weather Stations Within DCEW (Lower Weather - LW, Treeline - TL, Shingle Creek Ridge - SCR, Bogus Ridge Weather - BRW, and Lower Deer Point - LDP, from Lowest Elevation to Highest).

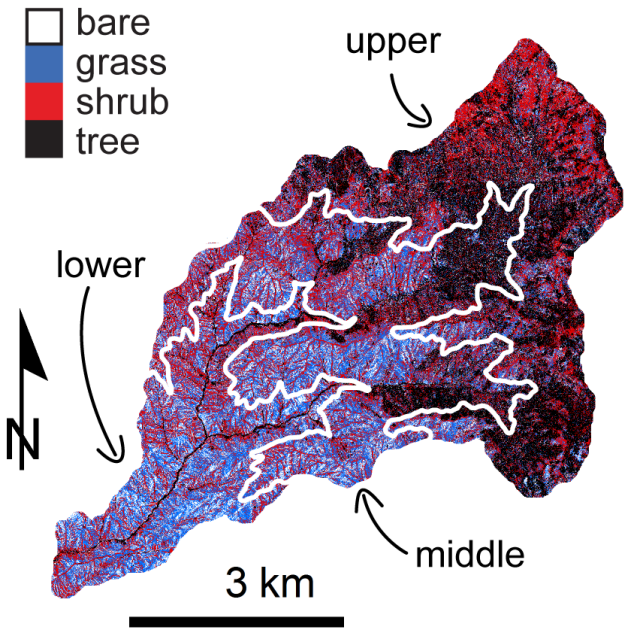

Figure 2: The Distribution of Vegetation Changes from Mostly Grasses and Shrubs in the Lower Elevations to Predominately Trees and Shrubs in the Upper

Elevations. The Middle Elevations Have Shrubs and Trees on their South-facing Hillslopes and Trees and Shrubs North-facing Hillslopes.

In our model, we used meteorological data from DCEW to inform our climate forcings, but not the actual topography from DCEW itself. DCEW has three main tributaries, but only the southernmost one has hillslopes that face directly north and south. Hillslopes within the other tributaries tend to be oriented in a Southwest- or Northeast-facing direction. In order to obtain an idealized landscape with primarily North- and South-facing hillslope facets for our study, we generated synthetic topography using Landlab's landscape evolution capabilities. We created a DEM with similar slope angles and hillslope curvatures to the topography in DCEW, but with predominantly north- and south-facing hillslopes. It is on this DEM that we ran the CATGRASS vegetation model, allowing us to generate results that are applicable to areas beyond the Boise Foothills that share the same ecology.

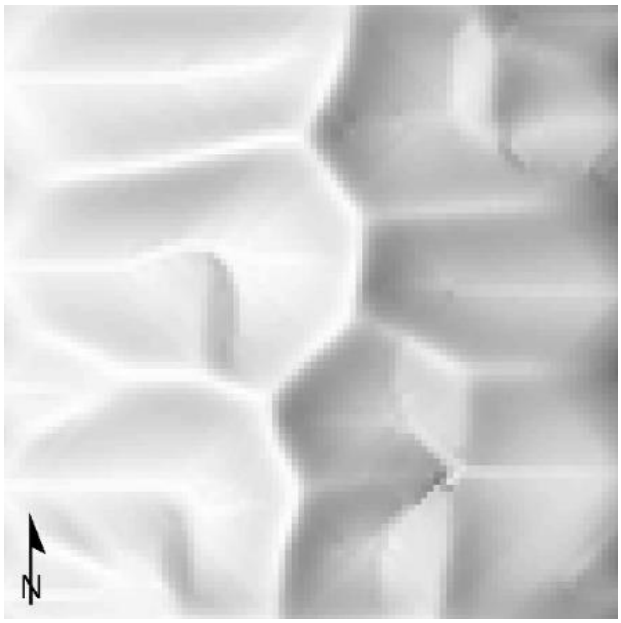

Figure 3: Hillshade of DEM Created with Landlab and Used as the Topography on Which Our Model Was Run.

Landlab

We used version 0.1 of Landlab. Landlab is written in Python, and we used Python 2.7.11 through Anaconda's Spyder interactive development environment (version 2.3.8). This was run on Microsoft Windows Server 2012 through Remote Desktop Services. Although the Landlab model is not well-suited to parallelization, we were able to improve computational efficiency on our terminal Windows server by running individual replicates from of each ensemble simultaneously, because they are independent. We used Open MPI (Message Passing Interface) to facilitate this.

Landlab divides its computational domain into nodes (G. E. Tucker et al., 2016), where only one PFT can occupy a node at a given time. At the beginning of each model run the nodes were seeded with a randomly chosen PFT from among trees, grasses, and shrubs. Seedlings can only establish themselves near a node containing an adult plant of the same PFT (with the distance at which an adult plant could establish a seedling dependent on PFT). For the purposes of our analysis, if a plant is established at a node, we count the area that node represents as fully occupied by that PFT regardless of plant health, age, biomass, or LAI (Leaf Area Index, a measurement of plant canopy). Nodes in our Landlab mesh (Fig. 3) represent an area of 1 m^2.

Each PFT has its own parameters to constrain their unique growing patterns (Hobley et al., 2017; Zhou et al., 2013)(Table 1). Trees have a lower maximum drought induced foliage loss rate (0.01 d-1) than shrubs and grasses (0.02 d-1). However, trees are more vulnerable to drought as seedlings than shrubs are, with drought resistance thresholds of 0.72 and 0.80 (dimensionless) respectively. We represented the high turnover of grasses through a background mortality parameter (likelihood of mortality in

any given year) of 0.05, comparted to the lower rate of 0.01 for trees and grasses, which are more stable than grasses once they have established themselves. Shrubs and trees also share a senescence coefficient of live biomass (0.002 d-1) that is lower than that of grass (0.012 d-1). CATGraSS uses the senescence coefficient of live biomass to calculate biomass dynamics; the high value assigned to grass reflects the extreme seasonality of its growth. Trees have deeper roots (1.3 m) than shrubs (0.5 m) and grasses (0.3 m), allowing them to tap into deeper sources of water than other PFTs and spread rapidly in climates with an abundance of water that can percolate to that depth.

Landlab controls recruitment of PFTs into nodes using a module developed from CATGraSS, which uses a rule based cellular automata approach to define the relationships between resource availability and vegetation health (Zhou et al., 2013). CATGraSS regulates vegetation growth through water availability (Caracciolo et al., 2014). We describe the most relevant equations that CATGraSS uses below.

CATGraSS defines water availability through a wide variety of variables related to the plant biophysical characteristics in each cell. These variables include daily radiation, rainfall, soil moisture, evapotranspiration (ET), net primary productivity (NPP), live and dead biomass for both above and belowground pools, and woody plant age, among others. A depth averaged water balance of the soil (Equation 1) constrains plant growth, where the rate of moisture change (captured by soil effective saturation (s), soil porosity (n), and effective rooting depth (Zr)), are balanced by the difference in the infiltration rate (Ia), actual evapotranspiration (ETa) and root zone leakage (D) (Eagleson, 1982; Rodriguez-Iturbe, 2000).

$$nZ_r \frac{ds}{dt} = I_a - ET_a(s) - D(s) \quad (1)$$

Plant water stress (ξ) is defined by the mean soil moisture content ($\bar{s}$), an evapotranspiration efficiency term based on depth average soil moisture in the root zone (β), and a parameter defining the nonlinear effects of water stress on plants (M, Equation $\xi = [1 - \beta(\bar{s})]^M$ (**2**)).

$$\xi = [1 - \beta(\bar{s})]^M \tag{2}$$

To calculate the water stress index (WSX), cumulative plant water stress (ξX) is normalized to the growing season length (Tseas, Equation $WS_X = \frac{\xi_X}{T_{seas}}$ (**3**), after (Porporato et al., 2001).

$$WS_X = \frac{\xi_X}{T_{seas}} \tag{3}$$

Plant live index (φX) is used to calculate seedling establishment probability (PE-X) (Caracciolo et al., 2014); each PFT has an individual maximum possible value of PE-X (Equations 4 and $P_{E-X} = min(\varphi_X, P_{E-X,max})$ (5), Porporato et al., 2001).

$$\varphi_X = 1 - WS_X \tag{4}$$

$$P_{E-X} = min(\varphi_X, P_{E-X,max}) \tag{5}$$

WS_X, is also used to calculate drought stress (PMd-X), along with a PFT-specific drought resistance threshold (θX, Equation $P_{Md-X} = WS_X - \theta_x$ (6) $P_{Md-X} = WS_X - \theta_x$ (6, Zhou et al., 2013).

$$P_{Md-X} = WS_X - \theta_x \tag{6}$$

Finally, drought stress (PMd-X) and plant age (PMa-X) define plant mortality (PM-X, Equation $P_{M-X} = P_{Md-X} + P_{Ma-X}$ (7, Zhou et al., 2013).

$$P_{M-X} = P_{Md-X} + P_{Ma-X} \quad (7)$$

Table 1: Parameterizations Used to Describe the Four Different Plant Functional Types in Our Model.

variable	bare	grass	shrub	tree
Soil Moisture				
full canopy interception capacity (mm)	1	1	1.5	2
root depth (m)	0.15	0.3	0.5	1.3
infiltration capacity of bare soil (mm/h)	20	20	20	20
infiltration capacity of vegetated soil (mm/h)	20	24	40	40
soil porosity	0.43	0.43	0.43	0.43
soil saturation degree at field capacity	0.56	0.56	0.56	0.56
soil saturation degree at stomatal closure	0.33	0.33	0.24	0.22
soil saturation degree at wilting point	0.13	0.13	0.13	0.15
soil saturation degree at hygroscopic point	0.1	0.1	0.1	0.1
deep percolation constant	13.8	13.8	13.8	13.8
Vegetation Dynamics				
water use efficiency KgCO2Kg-1H2O	0.01	0.01	0.0025	0.0045
specific leaf area for green/live biomass (m2 leaf g-1 DM)	0.0047	0.0047	0.004	0.004
specific leaf area for dead biomass (m2 leaf g-1 DM)	0.009	0.009	0.01	0.01
senescence coefficient of green/live biomass (d-1)	0.012	0.012	0.002	0.002
decay coefficient of aboveground dead biomass (d-1)	0.013	0.013	0.013	0.013
maximum drought induced foliage loss rate (d-1)	0.02	0.02	0.02	0.01
maximum leaf area index (m2/m2)	0.01	2	2	4
reference leaf area index (m2/m2)	0.01	2.88	2	4
Cellular Automaton Vegetation				
maximum establishment probability		0.35	0.2	0.25
allelopathic effect		2		
drought resistant threshold		0.62	0.8	0.72
drought resistant threshold (for a seedling)			0.64	0.64
background mortality probability		0.05	0.01	0.01
background mortality probability (for a seedling)			0.03	0.03
maximum age (year)			600	350
maximum age (year) (for a seedling)			18	18

Climate Forcings

Though the Treeline weather station measures data from one point within DCEW, applying that climate data to our whole synthetic DEM is acceptable because the actual

treeline catchment that our model represents does not vary significantly in elevation from the Treeline weather station site. Elevation is a strong control on precipitation, but our synthetic DEM falls within a narrow elevation band (less than 100 m) centered around 1610 m above sea level (the elevation of Treeline weather station). Due to this small change in elevation within our synthetic DEM, the effect of elevation on precipitation is small, and applying data derived from Treeline is assumed appropriate. Further, though radiation is highly aspect-dependent, our model generates an individual radiation value for each cell of the synthetic DEM, mitigating concerns that the aspect on which the weather station is located affected the model. We performed an analysis to confirm the model's sensitivity to changes in elevation at this scale, and outside of this section of the results all other model runs are performed with TL data, historical and future predictions.

Table 2: Summary Storm Statistics for Treeline Weather Station Within Dry Creek Experimental Watershed. These Statistics Were Used as the "Average" Climate Scenario Precipitation Data.

	storm duration (hrs)	inter-storm duration (hrs)	depth of rain (mm)
wet season	2.21	69.88	4.74
dry season	1.87	336.72	4.88

Landlab uses a stochastic weather generator that is parameterized by three storm statistics to characterize precipitation time series: average storm length, average inter-storm length, and average precipitation depth per storm. Given forcings for these variables, Landlab generates a sequence of storms that follow a Poisson arrival process (Laio et al., 2001), assuming an exponential distribution for each of these variables (Figure 5). This distribution introduces the random variability that can have a large impact on hydrology in arid ecosystems (Paschalis et al., 2016). We independently

calculated storm statistics for both wet and dry seasons (Table 2) based on meteorological data from Treeline Weather Station. To determine the cutoff date for wet and dry seasons, we calculated when precipitation had ended and then started again for the fifteen years on record for Treeline site. Apart from occasional summer storms, there was no precipitation in the summer. Rain ended around Julian Day (JD) 171 and began again around JD 270, so we chose those dates as our seasonal delineations. This introduces seasonality into the model, another important variable for arid ecosystems (D'Odorico et al., 2000)

Landlab calculates a potential evapotranspiration (PET) value that depends on vegetation type and is based on temperature and solar radiation. This PET value drives the ecohydrologic response of the landscape by defining how constrained the plants are by water availability. We used meteorological data from the Treeline weather station to generate PET values using the FAO-56 Penman-Monteith equation (R. G. Allen et al., 1998; Zotarelli et al., 2010). To obtain realistically varying PET values for grasses, shrubs, and trees, we assigned albedo values of 0.23, 0.14, and 0.08 respectively (Betts & Ball, 1997; Dirmhirn & Belt, 1971; C. L. Hanson, 2001).

We used nine climate scenarios, focused on the Treeline site within DCEW, to develop a suite of Psuedo Global Warming experiments that allowed us to determine the relative impact of precipitation and temperature change on landscape response (see Figure 4). These nine scenarios were created by increasing, decreasing, and holding steady our precipitation and temperature forcings. To create alternate temperature forcings we used MACAv2-METDATA climate forecasts (an ensemble of climate models, based on the Intergovernmental Panel on Climate Change's climate models (Moss et al., 2008)), but precipitation data from those projections exhibits significant

uncertainty and there is no clear trend in future total annual precipitation and/or storm characteristics. To mirror the most consistent trend in projections of future precipitation (a slight increase in mean annual precipitation by the end of the 21st century), we increased the precipitation depth from our historical storm statistics (these historical values are explained in more detail at the end of this section) by 10%. To do this we multiplied the average historical storm depth value by 0.9 and 1.1 to find a storm depth value for the decreased and increased precipitation climate scenarios respectively. While we are confident that a 10% change in precipitation is a reasonable possibility given the current generation of climate projection data (Hennessy, Gregory, & Mitchell, 1997; Karl & Knight, 1998; Kharin et al., 2007), in choosing to alter precipitation depth we are modifying only one of the variables that might effect that 10% change, namely intensity. Changing the timing of precipitation through different storm and inter-storm lengths could also achieve the same total rainfall, with a potentially large effect on vegetation. Future research should study this effect of changes in storm parameterization, as well as the importance of autumn versus spring precipitation, such as the work of (Bates et al., 2006; Crimmins, Crimmins, & Bertelsen, 2010).

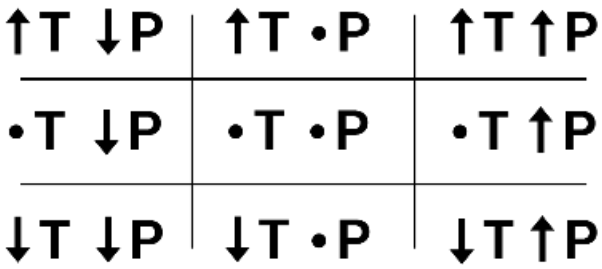

Figure 4: Nine Different Climate Scenarios Used to Test the Relative Sensitivity of Vegetation to Changes in Precipitation (P) and Temperature (T). Scenarios with No Change (a Single Dot) Were Based off Averaged Historical Data. Altered Precipitation and Temperature Scenarios Are Denoted by Up and Down Arrows.

To generate alternative temperature forcings, we used downscaled mean temperature values from MACAv2-METDATA (Abatzoglou, 2013). We used two sets of data from these models: one, from 2070-2100, which we refer to as the future projections. The other, from 1999-2014, we refer to as our historical data, or historical forecasts. We call the meteorological data collected at Treeline during the same period historical data as well. By comparing historical Treeline with historical forecast data from the pixel containing the Treeline catchment for the same time period, we are able to achieve a baseline difference between the two datasets, and use that difference to predict an analogous Treeline temperature to the future forecasts. We chose to use nine MACAv2-METDATA models with low error in both temperature and precipitation variables (Table 3). This was determined by Rupp et al.'s 2013 paper, where they evaluated an ensemble of climate models based on the Intergovernmental Panel on Climate Change's climate models against one another, and rated them based on their relative error compared to the ensemble's mean (Moss et al., 2008; Rupp et al., 2013; Sillmann et al., 2013). In this way, we could investigate the variability in potential future climate regimes by considering climate across nine different models, each with 29 years of variation.

Table 3: Relative Ensemble Error for Temperature of the Climate Models Used to Generate Temperature Forecasts (Rupp et al., 2013). We Only Used Models with Less Than 0.10 Error.

Model	T error
CanESM2	0.10
CCSM4	0.05
CISRO-Mk3-6-0	0.10
HadGEM2-CC	0.10
HadGEM2-ES	0.05
inmcm4	0.05
IPSL-CM5B-LR	0.10
MIROC-ESM	0.10
MIROC-ESM-CHEM	0.05

We spatially and temporally interpolated these MACAv2-METDATA models to find their average forecasted maximum and minimum daily temperature at Treeline Weather station. For both projected and historical MACAv2-METDATA data, we found the average high and low temperature of every day across the models, and used those data to find average monthly maximum and minimum differences between historical and forecasted values. Adding this difference to the historically measured Treeline data, we could obtain climate projections more appropriately constrained to our local weather stations' elevation, longitude, and latitude. The low temperature scenario was created by subtracting instead of adding the difference from the measured DCEW data. On average, the MACAv2-METDATA projections show an increase of a little over 3 degrees Celsius (Table 4). This number corresponds to a much larger change in the cooler months (averaging a 13.36% difference from December to February) than it does in the hotter months (averaging a 0.18% difference from July to September). With these newly adjusted temperature values, we recalculated seasonal PET for the climate scenarios that varied temperature.

Table 4: Average Historical Monthly Treeline Temperature (°C) and the Associated Value of Temperature Increase Generated Using the Macav2-METDATA Projections.

month	16-year TL mean (˚C)	MACA temperature increase (˚C)
January	0.33	3.62
February	-0.36	3.82
March	3.34	3.19
April	6.29	2.70
May	12.35	2.38
June	15.69	3.49
July	24.65	3.80
August	20.76	3.72
September	17.22	3.61
October	11.86	3.27

November	0.82	2.73
December	0.17	3.04

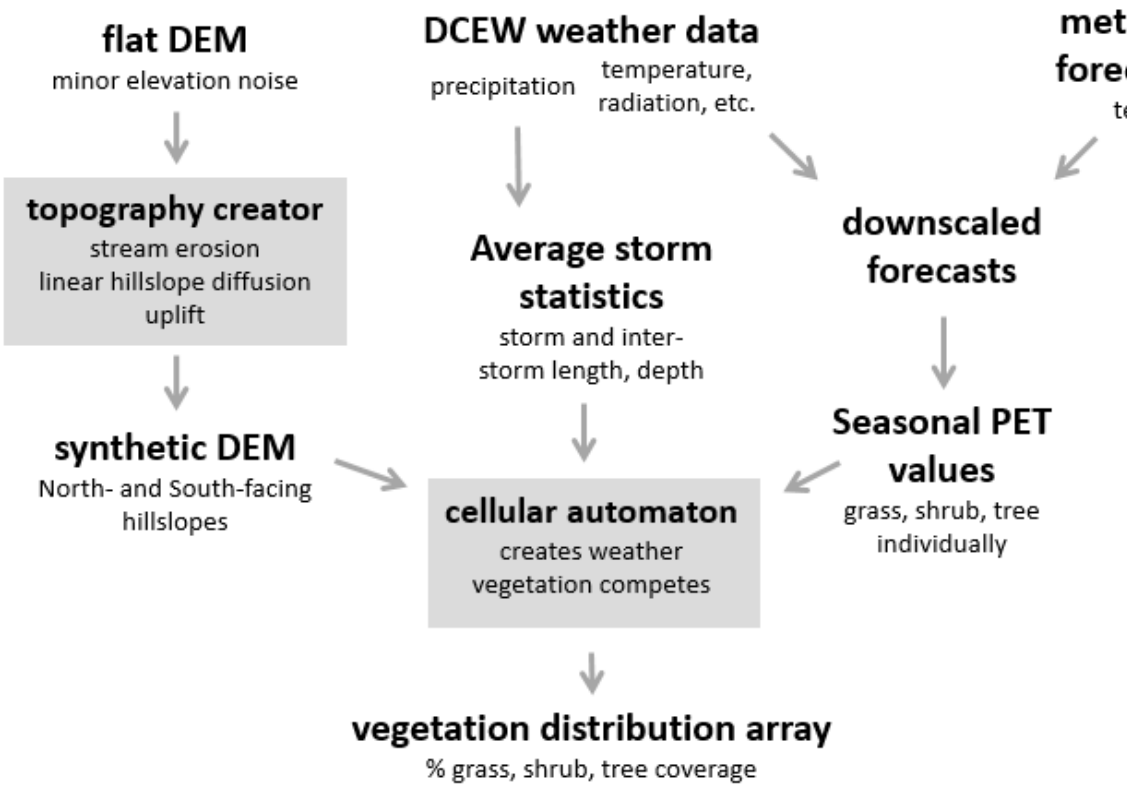

Figure 5: Flowchart Showing What Data Was Needed and How that Data Interacted to Create Our Final Output of Vegetation Arrays. Grey Boxes Are Steps that Took Place Using Landlab Tools. The Topography Creator is Discussed in Appendix B

Despite these efforts to reduce errors in our climactic data through the use of many predictive models, 30 years of data from each model, and interpolating to our location of interest, these data are still subject to irreducible uncertainties that cannot be adequately addressed here. We are comfortable, however, that this pseudo global warming (PGW) approach is consistent with modeling an idealized ecosystem that has a clear real-world analog, rather than modeling a specific real-world location in detail. We did, however, compare our outputs to observed distributions of PFTs within DCEW.

Because of extensive human management of DCEW that altered its distribution and density of native plants, this comparison is a broad-scale confirmation that the model reproduces a mix of grasses, shrubs, trees, and bare ground rather than an attempt to verify that the model reproduces specific metrics such as percent cover, etc. This comparison is located in Appendix D.

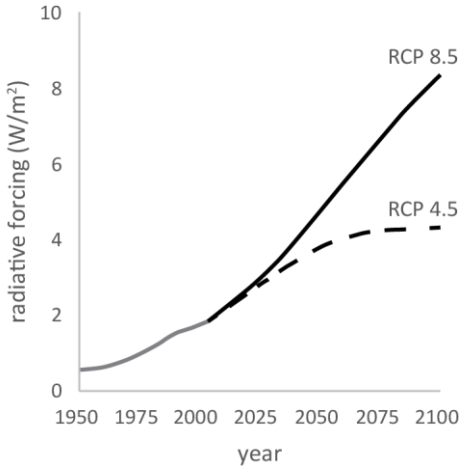

Figure 6: Comparison of the Two IPCC Climate Models Used in This Paper: RCP 4.5 And RCP 8.5. We Compare the Results of Our Model Using Both Projections; Our Analysis of Relative Plant Sensitivities is Based On RCP 8.5.

We ran our model using two of the IPCC's climate projections: Representative Concentration Pathways (RCP) 4.5 an RCP 8.5 (Figure 6). These IPCC projections model two potential climate futures that differ from one another based on projected increases (RCP 8.5) or stabilization (RCP 4.5) of greenhouse gases. RCP 8.5 is the more extreme, and more likely ((IPCC) Intergovernmental Panel on Climate Change, 2007), climate change scenario. The use of two different climate projections expanded the number of climate scenarios we ran from nine to eighteen. In our results, we compared the two projections, but ultimately base the conclusions of this paper on RCP 8.5.

Sensitivity Analysis of Model Parameters

We conducted a sensitivity analysis of our model results to minimize computation time. In this analysis, we focused on how long the model needs to run during a spin-up period before vegetation stabilized for a particular climate ensemble replicate (taking into account that some PFTs need longer than others to do so (Brubaker, 1986; Renwick & Rocca, 2015)) as well as the minimum number of ensemble replicates needed to provide reproducible statistics of vegetation cover for a given climate scenario.

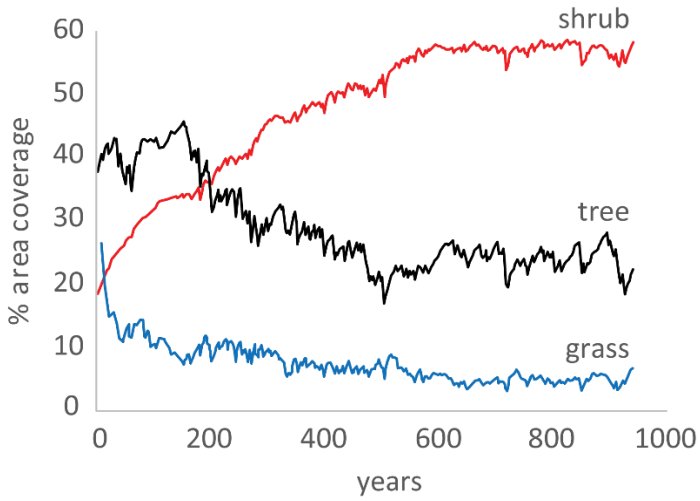

Figure 7: Example of How Vegetation Within Our Model Stabilizes Over Time. In This Example, Shrubs Increase in Area Covered, While Trees and Grasses Decrease. All Three Plant Functional Types Settle into a Steady Equilibrium Around 600 Years.

To find the minimum time our models needed to run, we ran 1000 replicates for 1000 years each. PFTs were distributed across each replicate in a unique way with a random seed. As the model ran, we determined the year that the percent area coverage for all three PFTs leveled off, indicating vegetation had reached an approximate dynamic equilibrium with the climate for that replicate. We defined vegetation stabilization using a 100-year rolling mean of the percent coverage for each PFT type. When the percent

coverage was within 5% of the rolling mean it was classified as stable. See Figure 7**Error! Reference source not found.** for an example of how vegetation coverage 'levels off' when it stabilizes.

We then used the above definition of 'time to vegetation stabilization' to test model variance between replicates run with the same climate and initial conditions. From a pool of 1000 replicates, we randomly chose a subsample of those replicates and found the subsample's average time until stabilization. The subsample varied in size from a single replicate to containing all 1000. At ensemble sizes of less than 300, time to stabilization varied widely, but above 500 replicates there was comparatively less variation in time to stabilization (Figure 8). We chose to run future ensemble replicates for 500 years each, a duration that is far above the average stabilization time in the ensemble experiment, to ensure each replicate equilibrates to the change in climate.

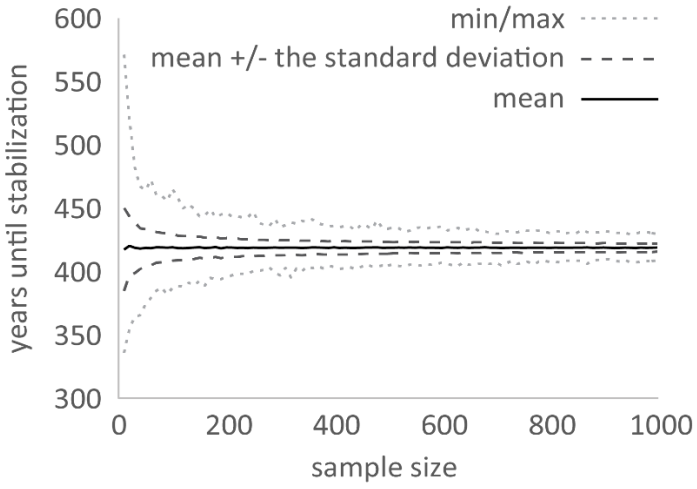

Figure 8: Using Grab Bags Ranging in Size From One Sample to 1000, We Investigated the Number of Replicates Needed Within an Ensemble to Ensure Statistical Robustness. Running an Ensemble of 500 Replicates for 500 Years Each Yields Certainty That Outliers Cannot Influence Our Data.

RESULTS

Quantification of Ensembles

Each climate scenario yielded an ensemble of 500 replicates, each with a unique terminal vegetation distribution that is simulated by Landlab after beginning from a different random initial condition. All scenarios were run to a steady state. Screening vegetation data by aspect, we used probability density functions (PDFs) to visualize PFT fractional cover on each aspect. South-facing aspects were any hillslopes in the 135 to 225 range (27% of the DEM's area); north-facing aspects were slopes between 315 and 45 (29% of the DEM's area). We used a nonparametric Kernel Density Function approach to estimate the underlying PDF. Specifically, we used an Epanechnikov kernel function and a bandwidth of 0.8 to generate these. This kernel and bandwidth value were chosen for their ability to accurately capture the shape of the data without amplifying insignificant variations or reducing the curve down to just the kernel shape (Figure 9, Figure 10). To more quantitatively describe the data, we further took the mode and standard deviation from each subset of vegetation type and aspect. The mode identifies the most common value to occur for each subset of the ensemble, or the value at the highest point of each PDF. To insure we only had one mode for each result, we rounded down the PFT coverage values to zero decimal places. There are 500 members in each ensemble, so this rounding only serves to distill the current statistics, not obscure nuance. This rounding means that when all PFT percent coverages are summed, the total ground covered will not always equal 100%. The standard deviation describes how consolidated

the various replicates are. Throughout this paper when we ascribe a given percent coverage of a PFT, we are referring to the mode of the ensemble.

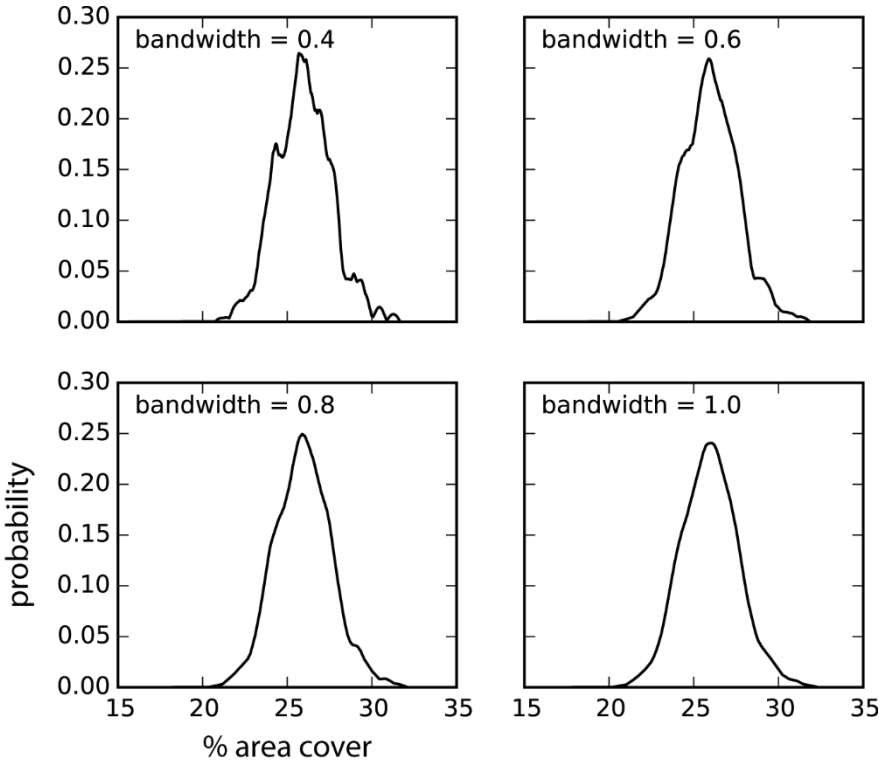

Figure 9: Example of Bandwidth Options for Our Probability Density Functions (Pdfs). Smaller Bandwidths Over-Emphasized Small Changes in PFT Coverage, Creating a Jagged Look (Such As the 0.4 Bandwidth Figure), While Large Bandwidths Smoothed Out Important Information (Such as the 1.0 Bandwidth Figure).

We would not have been able to fully evaluate our data without the use of the ensemble method. Just running the model once would give us an idea of what the results of a given climate would be on vegetation, but without replicates there is no way of knowing how representative that result is – we could randomly have a result that is the mean value, but it is also possible to yield a result located on the long tail of the distribution. Using the ensemble method frees our individual model runs from that uncertainty. Further, it also adds the value of showing us the shape of the distribution, allowing us to make conclusions about the stress levels of various PFTs.

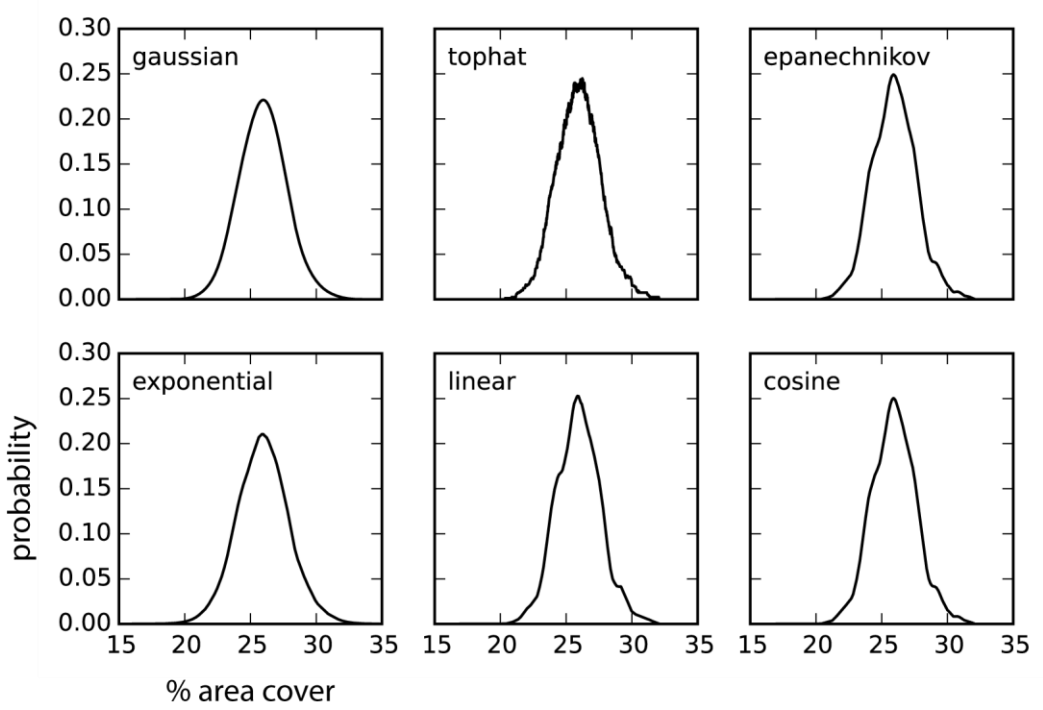

Figure 10: Six Different Kernel Options. Gaussian and Exponential Oversimplify the Data. Tophat Gives Too Much Weight to Small Variations. Epanechnikov, Linear, and Cosine All Resemble Each Other, Showing the Important Variation While Smoothing Out Noise

In our results, PDFs can be either short and fat or tall and skinny. A wide PDF indicates that the ensemble possesses significant variation among its ensemble replicates. This PDF will have a larger standard deviation, and indicates that those results might be straddling some sort of a climactic breaking point on an ecotone. For these climactic scenarios, a small change in precipitation or temperature has the potential to have an outsized impact on the ecosystem (Di Filippo et al., 2007; Macias et al., 2006; McAuliffe et al., 2014). By contrast, a thin, tall PDF has more consolidated values; the climate scenario that created this PDF would need dramatic alteration to see any significant change in percent PFT cover. These ecosystems are more resistant to changes in precipitation and temperature (and their impact on PET) alone. Using the ensemble method was critical to our ability to fully evaluate the results of our model.

Sensitivity Analysis of Elevation

To test the sensitivity of our model to changes in elevation, we ran it at five different locations within DCEW using unaltered historically measured DCEW weather station data. In this area, precipitation is extremely elevation dependent (Figure 11). This comparison of DCEW locations allowed us to verify that the model is sensitive to changes in precipitation that are associated with elevation, and confirmed that Treeline is the weather station closest to a tipping point, thus making it a good choice for our further analysis into relative sensitivities of PFTs.

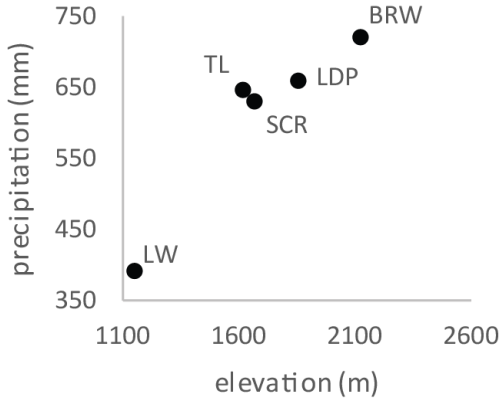

Figure 11: Precipitation Received by Each Weather Station Within DCEW, from Lowest Elevation to Highest (Lower Weather, Treeline, Shingle Creek Ridge, Lower Deer Point, Bogus Ridge Weather).

Throughout all elevations, east- and west-facing slopes had nearly identical vegetation distributions (Figure 12a). The largest variance between the two aspects occurred at Lower Weather, where east-facing shrubs covered 25% of the area compared to 21% on west-facing slopes. In general, though, the vegetation distributions for the two aspects are similar. The upper elevation simulations are all similar to each other (TL through BRW) on east and west slopes. Trees ranged from 50-56% coverage, shrubs 26-29%, bare 7-8%, and all grasses were 12%. By contrast, the lowest elevation (LW) has a significant plunge in tree coverage, to 4%. Bare ground and grasses increase to take their

place, to 30-34% coverage. This inversion is consistent with significantly less rain and higher temperatures.

North-facing slopes (Figure 12c) follow the same general trends as east and west slopes, with the exception of the LW elevation simulations. However, exceptionally, while there was slight variation among the upper elevation values on east and west slopes, on north-facing slopes all PFT values were identical from TL to BRW. At LW, north-facing slopes follow a similar reversal pattern in tree coverage as we observe on west and east slopes, although to a lesser extent. Trees decline to 21%. However, on north-facing slopes at this elevation, shrubs increase to fill up the area vacated by trees, to 46% coverage, instead of grasses and bare ground as we observed on east and west slopes. It is important to note that there is a large gap in elevation between LW and the next weather station, TL. This gap is where we observe the distribution of our PFTs changing the most quickly, potentially obscuring important detail.

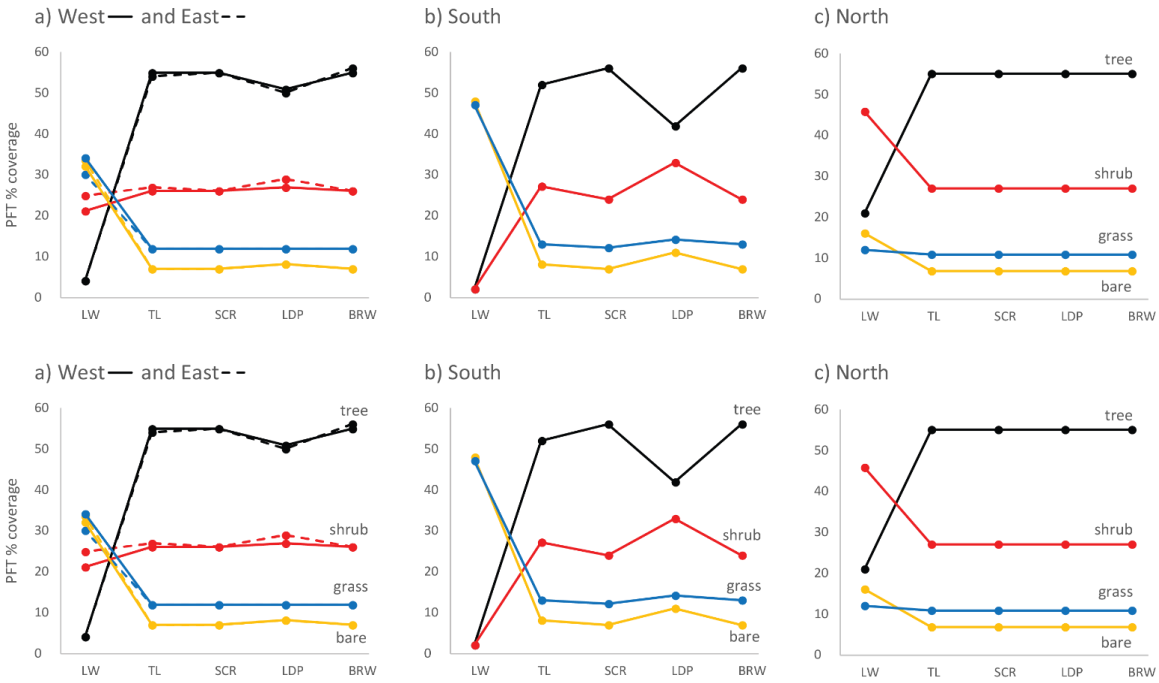

Figure 12: Plant Functional Type Distribution Across Elevation Distribution and Aspect. East and West Aspects Were Similar to Each Other. North-facing Slopes Follow the Same General Trends as East and West Slopes, With the Exception of the LW Elevation Simulations.

On south-facing slopes (Figure 12b), there are major differences between elevations. The lowest elevation stratifies even further than we observe on north, east, or west slopes. Trees and shrubs converge at 2% coverage, while grasses and bare ground take up 47% and 48% respectively. This pattern reverses itself in the upper elevations; trees and shrubs dominate, while grasses and bare ground cover area minimal ground.

In sum, the LW elevation is extremely dry. It receives enough precipitation to sustain shrubs on north-, east-, and west-facing slopes, but only grass on south-facing slopes. All other elevations receive at least 60% more historically measured precipitation than LW, and their vegetation is comprised of a high percentage of trees that reflect this. In general, these upper elevations are similar to one another, with the exception of LDP, which has less trees and more shrubs. As our climate dries and warms, we will start

seeing weather patterns most similar to that of LW, and our research question focuses on how the plants most at risk, those closest to an ecosystem threshold, react to that change.

RCP 4.5 Versus RCP 8.5

Using climate data from the TL historical and downscaled forecasts, we ran all nine climate scenarios using both RCP 4.5 and the more extreme and likely to occur RCP 8.5 climate projections, and then compared the two to determine the significance of using one projection versus the other. In this comparison, when looking at north-facing slopes (Figure 14, right), we saw no difference. Ensembles for both RCP 4.5 and 8.5 clustered closely around their mode (with an average standard deviation of 1.03 and 1.02 respectively for all vegetation and climate regimes, and the modes were virtually identical for the two RCP projections (

Table 5). However, on south-facing slopes we did observe discrepancies between RCP 4.5 and 8.5 (Figure 14, left). In high temperature scenarios, RCP 4.5 shrubs increased and grasses decreased in area coverage as compared with RCP 8.5. Contrary to expectations, the percent bare ground and tree coverage showed no differences between the two, and there is no corresponding discrepancy in the low temperature scenarios. Even with the PFT response to changes in climate on south-facing slopes, RCP 4.5 and 8.5 still showed minimal differences.

Table 5: The standard deviation and average of the modes of all climate scenarios for each aspect and RCP regime.

	bare		grass		shrub		tree	
	σ	average	σ	average	σ	average	σ	average
North 4.5	0.14	7.00	0.07	11.00	0.07	27.63	0.17	54.78
North 8.5	0.14	7.00	0.06	11.00	0.06	27.22	0.12	54.88
South 4.5	0.69	7.89	0.33	13.33	0.29	26.78	0.67	51.11
South 8.5	0.86	8.00	0.38	13.67	0.34	26.56	0.72	51.33

The were no differences between RCP 4.5 and 8.5 linked to changes in precipitation. This lack of contrast is logical, as we held precipitation constant in both RCP 4.8 and 8.5, with only a change in temperature. However, this finding does still yield information about the system: it tells us that a change in temperature alone is enough to force changes in a system, independent of precipitation levels. As RCP 8.5 is the climate scenario closest to what we expect to see in the future, we focus the rest of this paper on just the model scenarios using these data, with the exception of a section in the Discussion where we delve into the differences between the two RCP regimes.

North- Versus South-facing Slopes

North- and south-facing slopes reacted very differently to the same climate. North-facing slopes did not exhibit any change in vegetation distribution, regardless of variation in temperature or precipitation (see Table 6, Figure 14). On north-facing slopes, bare ground and grass held steady at 7% and 11% coverage respectively, and had standard deviations of less than one percent. Shrubs and trees displayed a slightly less condensed distribution, although with modes ranging from 27-28% and 54-55% respectively, there was essentially no difference in PFT distribution for any climate scenario on north aspects. This trend held constant for both the RCP 4.5 and the RCP 8.5 climate scenarios. On north-facing slopes, RCP 4.5 and RCP 8.5 scenarios had an

average standard deviation of 1.03 and 1.02 for all PFT types. These numbers reinforce that on these north-facing slopes there was very little change in PFT coverage between climate scenarios and RCP simulation.

Table 6: Percent Area Coverage for Each Plant Functional Type on North-facing Slopes in All Climate Scenarios. Numbers Given are the Mode of the Ensemble and Standard Deviation of the Mean.

		bare		grass		shrub		tree	
temp	precip	σ	mode	σ	mode	σ	mode	σ	mode
RCP 4.5									
increase	decrease	0.96	7	0.87	11	1.49	27	1.61	54
increase	average	0.63	7	0.72	11	1.41	27	1.26	55
increase	increase	0.63	7	0.7	11	1.29	28	1.18	55
average	decrease	0.66	7	0.82	11	1.43	28	1.4	55
average	average	0.59	7	0.74	11	1.34	28	1.24	55
average	increase	0.53	7	0.76	11	1.33	27	1.1	55
decrease	decrease	0.85	7	0.88	11	1.46	28	1.51	54
decrease	average	0.64	7	0.75	11	1.43	27, 28	1.24	55
decrease	increase	0.56	7	0.71	11	1.31	28	1.18	55
RCP 8.5									
increase	decrease	0.89	7	0.86	11	1.47	27	1.45	55
increase	average	0.83	7	0.85	11	1.37	27	1.4	55
increase	increase	0.82	7	0.8	11	1.3	27	1.26	55
average	decrease	0.6	7	0.82	11	1.39	27	1.34	55
average	average	0.64	7	0.77	11	1.28	27	1.26	55
average	increase	0.51	7	0.73	11	1.27	27	1.11	55
decrease	decrease	0.62	7	0.74	11	1.37	27	1.32	54
decrease	average	0.63	7	0.71	11	1.3	28	1.2	55
decrease	increase	0.51	7	0.73	11	1.32	28	1.13	54, 55

By contrast, there were differences between the south slopes in RCP 4.5 and 8.5 climate scenarios (Table 7, Figure 13, Figure 14), although they were small (less than 2% in all cases) compared to the standard deviations (0.96-4.46). In decreased temperature scenarios, trees grew better in RCP 8.5, where we decreased temperatures the most. In increased temperature scenarios, shrubs grew best in RCP 4.5, where we increased

temperature to a lesser extent than in the 8.5 scenarios. In neither of these cases is it entirely clear which PFT grew to take the extra space, or died off to make room, due to the error associated with losing decimal precision when calculating mode.

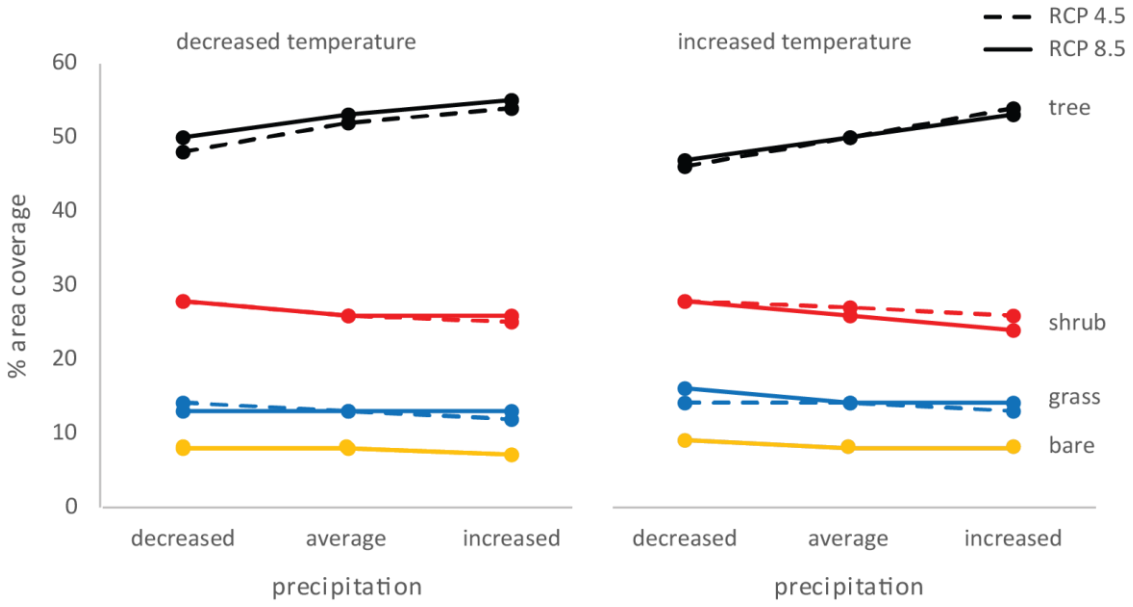

Figure 13: Comparison of RCP 4.5 (Dashed Line) And RCP 8.5 (Unbroken Line) Climate Scenarios on South-facing Hillslopes. All Data is from Either Decreased Temperature Scenarios (Left) or Increased Temperature Scenarios (Right). Though There are Small Differences (Less Than 2% in Either Direction), in General the Two Forcings Created Similar Resulting Ground Cover. Error! Reference source not found. **Contains the Exact Numbers**

Table 7: Percent Area Coverage for Each Plant Functional Type on South-facing Slopes in All Climate Scenarios. Numbers Given are the Mode of the Ensemble and Standard Deviation of the Mean.

		bare		grass		shrub		tree	
temp	precip	σ	mode	σ	mode	σ	mode	σ	mode
RCP 4.5									
increase	decrease	3.3	9	2.19	14	2.56	28	4.1	46
increase	average	2.65	8	1.69	14	2.21	27	3.52	50
increase	increase	1.96	8	1.34	13	1.83	26	2.66	54
average	decrease	2.54	8	1.85	14	2.29	28	3.77	49
average	average	1.94	8	1.49	13	2	28	2.78	52
average	increase	1.42	7	1.28	13	1.82	25	2.32	55
decrease	decrease	3.31	8	1.96	14	2.34	28	3.82	48
decrease	average	2.08	8	1.4	13	1.9	26	2.8	52
decrease	increase	1.55	7	1.32	12	1.7	25	2.39	54
RCP 8.5									
increase	decrease	3.91	9	2.38	16	2.73	28	4.46	47
increase	average	2.6	8	1.88	14	2.19	26	3.26	50
increase	increase	1.98	8	1.41	14	1.85	24	2.56	53
average	decrease	2.59	9	1.86	14	2.34	28	3.46	48
average	average	2.22	8	1.51	13	2.02	27	2.87	52
average	increase	1.55	7	1.22	13	1.72	26	2.42	54
decrease	decrease	2.53	8	1.63	13	2.13	28	3.42	50
decrease	average	1.48	8	1.46	13	1.83	26	2.65	53
decrease	increase	0.96	7	1.14	13	1.65	26	2.06	55

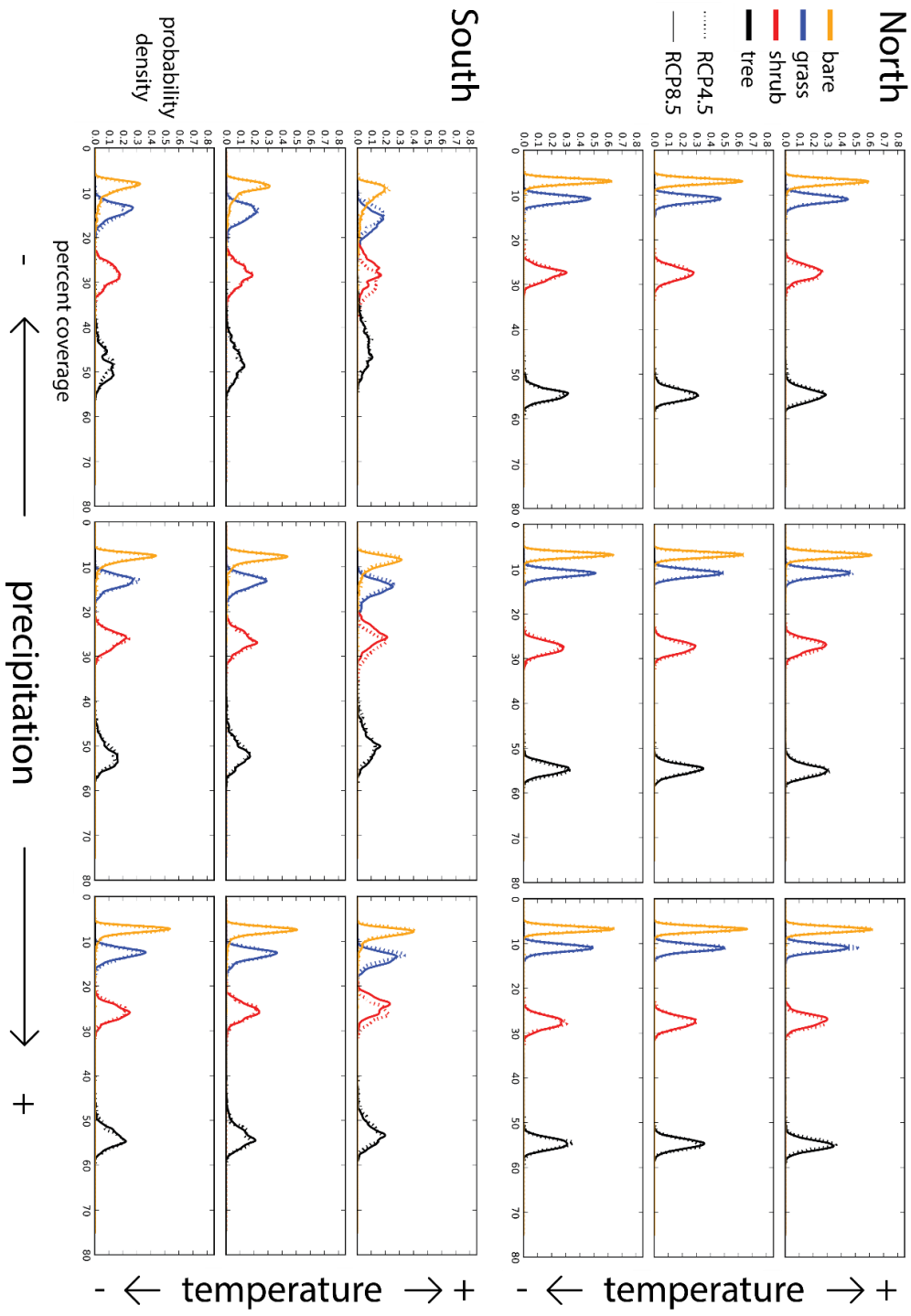

Figure 14: Probability Density Function of All Four Plant Functional Types On Both South (Left) And North Slopes (Right). The Dotted Lines Are for the RCP 4.5 Scenarios, and the Unbroken Lines Denote RCP 8.5. The Two Lines Are Impossible to Distinguish on All North-facing Slopes and Some South-facing Slopes Because They Lie on Top of Each Other. Here, the Same Plant Distribution Was Found Regardless of RCP Scenario Used.

While it is surprising that the modeled results showed no change in vegetation on north-facing slopes during our various climate scenarios, north- and south-facing slopes receive drastically different amounts of solar radiation at this slope angle and latitude (Figure 15). South- slopes receive a median of 1155 kWh/m2; north-facing slopes receive a median of 696 kWh/m2, although the distribution is trimodal due to slope curvature (Figure 16). The ridges are in sun most of the day and thus draw the most radiation; they are shown in the largest curve centered around 800 kWh/m2. The convex/planar parts of the hillslope are similar in shape to the ridges, but are lower down on the hillslope and thus are shadowed by opposite hillsides. These convex/planar areas receive around 420 kWh/m2. Finally, the shadowed concave valleys only obtain 180 kWh/m2. North-facing slopes at this location receive so little solar radiation that its relative importance drowns out any influence other variables might exert on vegetation patterns.

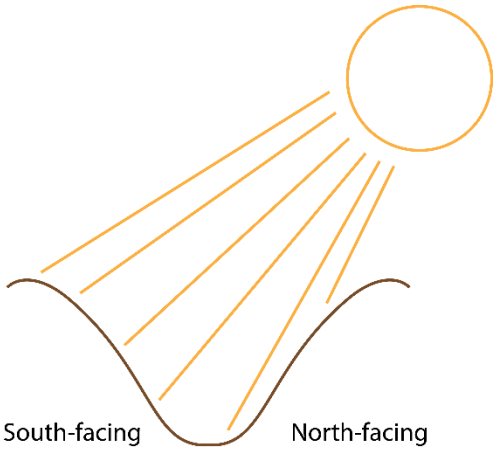

Figure 15: In the Northern Hemisphere, South-facing Slopes Collect Much More Sunlight Because They Directly Face the Sun, While North-facings Slopes Face Away from the Sun. Any Light That Does Reach a North-facing Slope Is Spread out Across a Larger Area than Sun That Reaches the South-facing Slope.

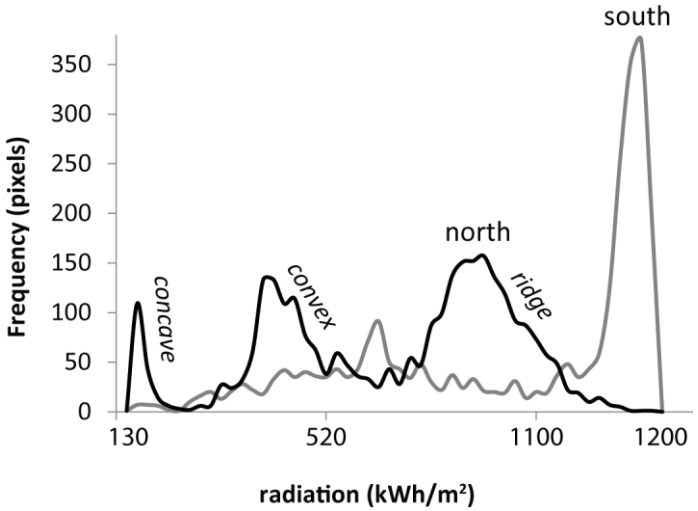

Figure 16: Radiation Received on North (Blue) Versus South Slopes (Orange). The North-facing Slope Receives a Trimodal Distribution of Radiation Due to the Curvature of the Slopes (Labeled Concave, Convex, and Ridge).

South-facing Slopes

In contrast with north-facing slopes, the vegetation on south-facing aspects was highly reactive to changes in climate (Table 5). In climate scenarios with less rain, the percentage of area covered by trees was 3-4% less than the cover in scenarios with average precipitation, while shrub coverage increased to fill in that area. The converse was true of high precipitation scenarios - tree coverage in high precipitation climate regimes converged around 53-55% (σ = 2.06-2.56), as opposed to low precipitation regimes whose tree cover was 47-50% but with a large σ of 3.42-4.46. In the low precipitation climate scenarios, where tree coverage decreased, shrub and grass coverage increased to fill in the uncovered ground. In all low-precipitation scenarios, shrub coverage was 28%, an increase of 1-4% over the correlated high and average precipitation scenarios.

Temperature exacerbated the trend of limited water limiting tree growth; the climate scenario with low precipitation and high temperatures had the lowest recorded

tree cover, 47% ($\sigma = 4.46$), of all scenarios. However, high precipitation decreased or even negated the effects of temperature on PFT distributions. The temperature-driven difference in tree coverage was 2% for these high precipitation regimes, compared with a 3% temperature-driven difference in average tree coverage for low-precipitation climate scenarios. The standard deviation of the average tree coverage also changed between high and low precipitation scenarios. Tree distribution in high precipitation scenarios were more tightly clustered around the mean ($\sigma = 2.06$-2.56), while in low precipitation scenarios tree percent cover displayed more variability ($\sigma = 3.42$-4.46). Similarly, grass percent coverage in low precipitation, increased temperature scenarios was 2% higher than in the high precipitation, increased temperature scenarios (16% versus 14%). This trend held, although diminished to 1% instead of 2% in the average temperature scenarios. In low temperature scenarios, however, there was no difference in grass coverage (13%) associated with any change in precipitation.

DISCUSSION

Nature has inherent disturbances, which will not by definition be visible in a model run to a steady-state. We only see the broad tendencies of the simulated vegetation distribution of PFTs once they have fully adjusted to a particular climate. In reality, however, climate can change at rates much faster than PFTs can adapt and may also exhibit influences of disturbances and limitations in availability of nutrients that are not presently captured in models like Landlab. Further, in our model no changes take place aside from climate, ignoring disturbances such as invasive species (which commonly compete with shrubs and grasses), fires, or anthropogenic influences. This makes it impossible to correlate our findings with real-world data in a way that allows specific quantitative predictions. However, this does not mean modeling is only useful for theoretical explorations. Instead of estimating exact changes in PFT at a given aspect and location, we infer the direction of change, and use differences in magnitude to make conclusions on the relative importance of temperature and precipitation on plant life in semi-arid ecosystems.

North- Versus South-facing Slopes

We observed differences in how south and north slopes responded to changes in climate. South-facing slopes were more reactive to changes in climate because they are at the edge of a tipping point and are thus more sensitive to small changes. North slopes do not lie within an ecotone and would need large changes in both temperature and precipitation to observe changes in PFT distribution. These northern aspects would need

a much larger change in climate than we will see with even RCP 8.5 to see significant changes in vegetation type. The narrow distributions and low standard deviations for the ensembles on north-aspects reflect this stable ecosystem. Large differences in hydrography between the microclimates on north- and south-facing hillslopes are not atypical (Geroy et al., 2011), but the magnitude of this difference in striking.

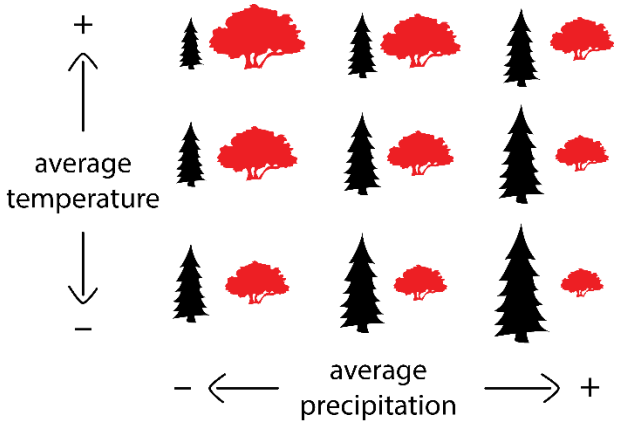

Figure 17: Results for South-Facing Hillslopes (Not to Exact Scale). Trees Covered More Area in Wet, Cold Scenarios; Shrubs Grew Better in Dry, Hot Scenarios.

South-facing Slopes

Unsurprisingly, in climate scenarios with less rain we observed less tree growth on south-facing slopes, and by simultaneously increasing temperatures our model grew even less trees (Figure 17). However, in high-precipitation regimes the distributions of trees were grouped tightly together, showing that temperature had less of an effect in arid ecosystems than precipitation. While a small change in temperature might expose our finding to claims that temperature was not altered enough to have a difference, our climate scenarios increased temperature by a large percentage in the wet months (up to 18.36% in December).

Previous research also supports precipitation being the dominant control in arid ecosystems. Villalba & Veblen, 1998 found that a sharp decrease in a single year's

annual precipitation was a more important factor for tree mortality than multi-year warm, dry periods, although (Swetnam & Betancourt, 1998) showed that multi-year droughts were important for determining the structure of an arid ecosystem, with its longer generation times. These findings contrast with research done at higher elevations, which have been found to be more sensitive to temperature (Rossi et al., 2008). (Suarez et al., 2015) and (Case & Peterson, 2007) found that trees were more sensitive to higher temperatures than to limited water at their more mesic, upper elevation sites and that they were more sensitive to limited water in lower elevation sites. In our system, precipitation is the dominant control, while these researchers' mesic locations receive enough water that temperature is the most important, allowing the two findings to exist without inconsistency.

Consistently with our results, (Grossiord et al., 2017) demonstrate that Pinus edulis, a tree species common to North America that grows in semi-arid locations, exhibits plastic changes in response to drought, but has only a moderate response to an increase in temperature alone. Unlike our findings, however, (Garcia-Forner et al., 2016; Grossiord et al., 2017) found no compounding effect of increased drought in addition to increased temperatures. This discrepancy could simply be the result of differing timescales; while a change in climate might not have a measurable response in vegetation in the short term (such as (Bates et al., 2006) observed in the initial years of their study), or be confounded by previous conditions, this climate pattern can have a large enough effect on tree survival to change species distribution in a climate scenario that has been run until steady state.

This finding highlights several new directions for future research. In our study, we only altered the depth of precipitation, not the timing. This is not a completely realistic scenario, given that changes in timing and intensity of precipitation are extremely likely (Kharin et al., 2007; Zhang et al., 2007). Spring drought should exaggerate our findings that water limitation decreases tree growth (L. D. L. Anderegg, W. R. L Anderegg, & Berry, 2013; Lebourgeois et al., 2012; Suarez et al., 2015), but could also lead to declines in shrubs that we did not observe in our work (Bates et al., 2006). Future research should continue this line of questioning by testing the sensitivity of our results to similar temporal changes in rain distribution, such as keeping the same total precipitation, but changing the timing to occur earlier in the year, or in short, intense bursts. This would allow the research to expand beyond hypothetical tests of PFT sensitivities to modeling how plants will respond to the expected changes in climate.

RCP 4.5 Versus RCP 8.5

Though we did see a slight difference in values between RCP 4.5 and 8.5 climate scenarios, these results were not stark. RCP 8.5 scenarios had their temperatures exaggerated compared to those that used RCP 4.5, so temperature-dependent trends should have similarly been exaggerated. When we looked at just our RCP 8.5 model runs, in low-temperature, high-precipitation scenarios trees did best at the expense of shrubs, and to a lesser extent grasses. Following this pattern, we observed 1-2% less trees in the decreased temperature RCP 4.5 scenarios than in the decreased temperature RCP 8.5 scenarios (Figure 13, left). However, grasses and shrubs did not grow as expected. In the decreased temperature, increased precipitation scenarios, RCP 8.5 shrubs and grasses both outperformed their counterpoints from RCP 4.5, if only by 1%. This incongruity can

partly be attributed to rounding errors; when we calculated the mode we used only whole numbers to represent each replicate's percent PFT coverage. Rounding eliminated double and triple mode values, but increased our resolution to a larger value than the standard deviation of the ensemble. Since the incongruous values are only unexpected by 1%, we can accredit this unexpected finding to lack of resolution. Further, the average standard deviation for both RCP 4.5 and RCP 8.5 was just above 1 (1.03 and 1.02 respectively), reinforcing that the two scenarios were extremely similar, and differences between the two can be attributed to the variation within the samples.

Model Forcings and Parameterization

There are some drawbacks in the way we set up the model, and these deficiencies are a useful starting point for future work. These deficiencies effected the growth of grasses more than the other PFTs. We expected to see grass distribution expand along with shrubs to take the place of trees in low-precipitation, high-temperature climate scenarios (Hufkens et al., 2016; Wilcox et al., 2012). While we did observe that pattern, shrubs expanded to replace trees at a greater rate than grasses did. This discrepancy between our observations and expectations can be explained through an exploration of our model weaknesses.

In our model, we kept the wet and dry seasons stable in length regardless of climate scenario, only changing precipitation intensity. The timing of this seasonality has differing effects on the various PFTs (W. R. L. Anderegg, Kane, & L. D. L. Anderegg, 2013, 2013; Bates et al., 2006; Chimner et al., 2010; Schwinning et al., 2005b). Grasses need a season with regular (as opposed to infrequent but intense) precipitation to compete with trees and shrubs, which can better withstand long periods of drought through

reliance on more stable deep water sources (Brunsell, Nippert, & Buck, 2013; Chou et al., 2008; Schwinning et al., 2005a). Future sensitivity analysis on PFT growth with regard to the timing and length of these seasons would be useful, as well as altering the intensity and length of rainstorms (Sun et al., 2007). These changes in intensity and timing are closer to how weather patterns will change (Easterling et al., 2000; Huntington, 2006; Knapp et al., 2008), and can have an outsized impact on grasses (Fay et al., 2003), which rely on the upper layers of soil which are most responsive to changes in precipitation timing (Knapp et al., 2002). If we held precipitation and temperature stable within our current RCP 8.5 scenario but increasing the length of the dry season we would likely see the expected increase in grasses, whereas changes in storm intensity with longer periods between storms would decrease grass coverage (Knapp et al., 2002).Research building from this project should first focus on studying the intensity and duration of storms.

Soil depth is an important control on vegetation growth that we did not investigate. Instead, we held it constant across our topography. As discussed in the introduction, vegetation growth and other factors create a feedback loop that causes soil to develop more deeply on north-facing slopes than south-facing ones. This asymmetry could decrease the expression of the patterns we observed, where north-facing slopes were susceptible to climate change but south-facing slopes were not. Instead, greater soil depth (and the associated greater water storage capability (Smith et al., 2011)) might insulate trees from some of the effects of drought, allowing them to be more competitive than they were in our high temperature, low precipitation simulations.

Rooting depth is another parameter that would be useful to study further. In our model, grasses have a rooting depth of 0.3 m, shrubs 0.5 m, and trees 1.3 m. However,

the rooting structure of shrubs can be more complicated than a single number to represent depth. While the majority of the root system of Artemisia tridentata is comprised of a shallow, diffuse root network, they also have a taproot that can reach up to 1.8-2 m in depth (Klepper, Gano, & Cadwell, 1985; Tabler, 1964). Our expectation that shrubs would thrive in low-water scenarios at the expense of trees was validated, but it is possible that our results underestimate the extent of this trend. If we had incorporated into our model a more complex root system, or even simply increased the shrub rooting depth, would shrubs have expanded at an even greater rate than observed in low-precipitation scenarios, and grasses correspondingly decreased their area coverage? This, also, would be a useful direction for future studies.

Further, it would be useful to look at the interplay of the parameters discussed above. A deep tap root allows *A. tridentata* to thrive at the expense of herbaceous species such as grasses (Darrouzet-Nardi, D'Antonio, & Dawson, 2006), and thus utilize deep soil water from intense and infrequent rainfall. (Bates et al., 2006) show this advantage may be moot in areas with shallow soil. How, then does this interplay of various species' adaptations play out in areas with variable soil depth, such as is observed in many transects of north- to south-facing hillslopes?

Finally, our model itself does not constrain all possible variables that influence plant growth. This is not a reasonable goal, but other model chose to approach this issue by emphasizing variables that are not included in Landlab and leaving out ones that are central to Landlab's functionality. An example of this is (Paschalis et al., 2016), whose model has very detailed hydrological processes and vegetation structure, but works on a temporal scale that is much shorter than what we explore in this paper. Of particular

interest in future extensions of this work is the potential role that the coupled biogeochemical processes potentially play in constraining vegetation growth and health. Soil microbial ecosystems may be more susceptible to changes in precipitation and temperature and may exert an influence on the availability of, for example, nitrogen on plant growth. At present, these biogeochemical processes are not captured within Landlab, although they are known to be significant in controlling ecosystem productivity. As such, the addition of computationally efficient representation of biogeochemical processes coupled to the water and energy balance provide an opportunity to extend the present work using the same modeling framework and experimental approach.

CONCLUSION

In this paper, we presented an application of the new bioecological landscape model Landlab in a semi-arid ecosystem. We ran 500 replicates of nine climate scenarios, for two different ICPP predictions (RCP 4.5 and 8.5). This modeling does not give us the exact number of a given PFT at a given location, but instead tells us the relative sensitivity of these PFTs to precipitation versus temperature. We showed that, in this ecosystem, trees are the most sensitive PFT to changes in climate. Trees die off in greater numbers at higher temperatures and thrive in lower temperature, wetter environments, while conversely shrubs and grasses increase their distributions in hotter and more dry environments. Temperature is important to all species, but we show that precipitation is the limiting variable in this ecosystem, controlling if temperature will have an impact or not. In high precipitation regimes, temperature has little effect, while in low precipitation regimes an increase in temperature will adversely impact tree species and the reverse is true of low precipitation and temperature scenarios. As our climate changes in accordance with RCP 8.5 predictions, we should be careful of our stewardship of our tree species, and to a lesser extent some shrubs.

Humans will increasingly have an outsized effect on semi-arid ecosystems as well, compounding the stress trees are already feeling due to climate change. Logging, invasive species, fires and the subsequent flooding and landslides associated with fires (among other human-caused disturbances) are all likely to change the composition of

plant species on the Great Basin region in the coming years, and land managers should be alert to these dangers as they act as stewards of the land.

REFERENCES

Abatzoglou, J. T. (2013). Development of gridded surface meteorological data for ecological applications and modelling. *International Journal of Climatology*, *33*(1), 121–131. https://doi.org/10.1002/joc.3413

Abatzoglou, J. T., & Brown, T. J. (2012). A comparison of statistical downscaling methods suited for wildfire applications. *International Journal of Climatology*, *32*(5), 772–780. https://doi.org/10.1002/joc.2312

Abrahams, A. D., Parsons, A. J., & Wainwright, J. (1995). Effects of vegetation change on interrill runoff and erosion, Walnut Gulch, southern Arizona. *Geomorphology*, *13*(1–4), 37–48. https://doi.org/10.1016/0169-555X(95)00027-3

Allen, R. G., Pereira, L. S., Raes, D., Smith, M., & others. (1998). Crop evapotranspiration-Guidelines for computing crop water requirements-FAO Irrigation and drainage paper 56. *FAO, Rome*, *300*(9), D05109.

Anderegg, L. D. L., Anderegg, W. R. L., & Berry, J. A. (2013). Not all droughts are created equal: translating meteorological drought into woody plant mortality. *Tree Physiology*, *33*(7), 672–683. https://doi.org/10.1093/treephys/tpt044

Anderegg, W. R. L., Kane, J. M., & Anderegg, L. D. L. (2013). Consequences of widespread tree mortality triggered by drought and temperature stress. *Nature Climate Change*, *3*(1), 30–36. https://doi.org/10.1038/nclimate1635

Anderson, B. T., McNamara, J. P., Marshall, H.-P., & Flores, A. N. (2014). Insights into the physical processes controlling correlations between snow distribution and terrain properties. *Water Resources Research*, *50*(6), 4545–4563. https://doi.org/10.1002/2013WR013714

Bates, J. D., Svejcar, T., Miller, R. F., & Angell, R. A. (2006). The effects of precipitation timing on sagebrush steppe vegetation. *Journal of Arid Environments*, *64*(4), 670–697. https://doi.org/10.1016/j.jaridenv.2005.06.026

Betts, A. K., & Ball, J. H. (1997). Albedo over the boreal forest. *Journal of Geophysical Research: Atmospheres*, *102*(D24), 28901–28909. https://doi.org/10.1029/96JD03876

Brubaker, L. B. (1986). Responses of Tree Populations to Climatic Change. *Vegetation*, *67*(2), 119–130.

Brunsell, N. A., Nippert, J. B., & Buck, T. L. (2013). Impacts of seasonality and surface heterogeneity on water-use efficiency in mesic grasslands: WATER-USE EFFICIENCY IN MESIC GRASSLANDS. *Ecohydrology*, n/a-n/a. https://doi.org/10.1002/eco.1455

Burnett, B. N., Meyer, G. A., & McFadden, L. D. (2008). Aspect-related microclimatic influences on slope forms and processes, northeastern Arizona. *Journal of Geophysical Research: Earth Surface*, *113*(F3), F03002. https://doi.org/10.1029/2007JF000789

Burroughs, E. R., & Thomas, B. R. (1977). *Declining root strength in Douglas-fir after felling as a factor in slope stability* (No. Research Paper INT-190) (p. 27). Washington, D.C.: United States Forest Service. Retrieved from http://agris.fao.org/agris-search/search.do?recordID=US201300717302

Caracciolo, D., Noto, L. V., Istanbulluoglu, E., Fatichi, S., & Zhou, X. (2014). Climate change and Ecotone boundaries: Insights from a cellular automata ecohydrology model in a Mediterranean catchment with topography controlled vegetation patterns. *Advances in Water Resources*, *73*, 159–175. https://doi.org/10.1016/j.advwatres.2014.08.001

Case, M. J., & Peterson, D. L. (2007). Growth-climate Relations of Lodgepole Pine in the North Cascades National Park, Washington. *Northwest Science*, *81*(1), 62–75. https://doi.org/10.3955/0029-344X-81.1.62

Caylor, K. K., Manfreda, S., & Rodriguez-Iturbe, I. (2005). On the coupled geomorphological and ecohydrological organization of river basins. *Advances in Water Resources*, *28*(1), 69–86. https://doi.org/10.1016/j.advwatres.2004.08.013

Chimner, R. A., Welker, J. M., Morgan, J., LeCain, D., & Reeder, J. (2010). Experimental manipulations of winter snow and summer rain influence ecosystem carbon cycling in a mixed-grass prairie, Wyoming, USA. *Ecohydrology*, *3*(3), 284–293. https://doi.org/10.1002/eco.106

Chou, W. W., Silver, W. L., Jackson, R. D., Thompson, A. W., & Allen-Diaz, B. (2008). The sensitivity of annual grassland carbon cycling to the quantity and timing of rainfall. *Global Change Biology*, *14*(6), 1382–1394. https://doi.org/10.1111/j.1365-2486.2008.01572.x

Collins, D. B. G., & Bras, R. L. (2008). Climatic control of sediment yield in dry lands following climate and land cover change. *Water Resources Research*, *44*(10), W10405. https://doi.org/10.1029/2007WR006474

Crimmins, T. M., Crimmins, M. A., & Bertelsen, C. D. (2010). Complex responses to climate drivers in onset of spring flowering across a semi-arid elevation gradient. *Journal of Ecology*, *98*(5), 1042–1051.

Darrouzet-Nardi, A., D'Antonio, C. M., & Dawson, T. E. (2006). Depth of water acquisition by invading shrubs and resident herbs in a Sierra Nevada meadow. *Plant and Soil*, *285*(1/2), 31–43. https://doi.org/10.1007/s11104-005-4453-z

DeGraff, J. V. (1979). Initiation of shallow mass movement by vegetative-type conversion. *Geology*, *7*(9), 426–429. https://doi.org/10.1130/0091-7613(1979)7<426:IOSMMB>2.0.CO;2

Di Filippo, A., Biondi, F., Čufar, K., De Luis, M., Grabner, M., Maugeri, M., … Piovesan, G. (2007). Bioclimatology of beech (Fagus sylvatica L.) in the Eastern Alps: spatial and altitudinal climatic signals identified through a tree-ring network. *Journal of Biogeography*, *34*(11), 1873–1892. https://doi.org/10.1111/j.1365-2699.2007.01747.x

Dirmhirn, I., & Belt, G. H. (1971). Variation of albedo of selected sagebrush range in the intermountain region. *Agricultural Meteorology*, *9*, 51–61. https://doi.org/10.1016/0002-1571(71)90006-9

D'Odorico, P., Ridolfi, L., Porporato, A., & Rodriguez-Iturbe, I. (2000). Preferential states of seasonal soil moisture: The impact of climate fluctuations. *Water Resources Research*, *36*(8), 2209–2219. https://doi.org/10.1029/2000WR900103

Fay, P. A., Carlisle, J. D., Knapp, A. K., Blair, J. M., & Collins, S. L. (2003). Productivity responses to altered rainfall patterns in a C4-dominated grassland. *Oecologia*, *137*(2), 245–251. https://doi.org/10.1007/s00442-003-1331-3

Garcia-Forner, N., Adams, H. D., Sevanto, S., Collins, A. D., Dickman, L. T., Hudson, P. J., … Mcdowell, N. G. (2016). Responses of two semiarid conifer tree species to reduced precipitation and warming reveal new perspectives for stomatal regulation. *Plant, Cell & Environment*, *39*(1), 38–49. https://doi.org/10.1111/pce.12588

Geroy, I. J., Gribb, M. M., Marshall, H. P., Chandler, D. G., Benner, S. G., & McNamara, J. P. (2011). Aspect influences on soil water retention and storage. *Hydrological Processes*, *25*(25), 3836–3842. https://doi.org/10.1002/hyp.8281

Grossiord, C., Sevanto, S., Adams, H. D., Collins, A. D., Dickman, L. T., McBranch, N., … McDowell, N. G. (2017). Precipitation, not air temperature, drives functional responses of trees in semi-arid ecosystems. *Journal of Ecology*, *105*(1), 163–175. https://doi.org/10.1111/1365-2745.12662

Hanson, C., & Johnson, G. (2001). Spatial and Temporal Precipitation Characteristics in Southwest Idaho.

Hanson, C. L. (2001). Clear-sky albedo measured at seven rangeland sites in southwest Idaho. *Journal of Hydrologic Engineering*, *6*(6), 532–534. https://doi.org/10.1061/(ASCE)1084-0699(2001)6:6(532)

Hennessy, K. J., Gregory, J. M., & Mitchell, J. F. B. (1997). Changes in daily precipitation under enhanced greenhouse conditions. *Climate Dynamics*, *13*(9), 667–680. https://doi.org/10.1007/s003820050189

Hobley, D. E. J., Adams, J. M., Nudurupati, S. S., Hutton, E. W. H., Gasparini, N. M., Istanbulluoglu, E., & Tucker, G. E. (2017). Creative computing with Landlab: an open-source toolkit for building, coupling, and exploring two-dimensional numerical models of Earth-surface dynamics. *Earth Surface Dynamics*, *5*(1), 21–46. https://doi.org/https://doi.org/10.5194/esurf-5-21-2017

Hufkens, K., Keenan, T. F., Flanagan, L. B., Scott, R. L., Bernacchi, C. J., Joo, E., … Richardson, A. D. (2016). Productivity of North American grasslands is increased under future climate scenarios despite rising aridity. *Nature Climate Change*. https://doi.org/10.1038/nclimate2942

Huntington, T. G. (2006). Evidence for intensification of the global water cycle: Review and synthesis. *Journal of Hydrology*, *319*(1–4), 83–95. https://doi.org/10.1016/j.jhydrol.2005.07.003

(IPCC) Intergovernmental Panel on Climate Change. (2007). Climate Change 2007: The Physical Science Basis. Summary for Policymakers. New York: Cambridge University Press. Retrieved from www.ipcc.ch/ipccreports/ ar4-wg1.htm

Istanbulluoglu, E., Yetemen, O., Vivoni, E. R., Gutiérrez-Jurado, H. A., & Bras, R. L. (2008). Eco-geomorphic implications of hillslope aspect: Inferences from analysis of landscape morphology in central New Mexico. *Geophysical Research Letters*, *35*(14), L14403. https://doi.org/10.1029/2008GL034477

Istanbulluoglu, E., Tarboton, D. G., Pack, R. T., & Luce, C. H. (2004). Modeling of the interactions between forest vegetation, disturbances, and sediment yields. *Journal of Geophysical Research: Earth Surface, 109*(F1), F01009. https://doi.org/10.1029/2003JF000041

Ivanov, V. Y., Bras, R. L., & Vivoni, E. R. (2008). Vegetation-hydrology dynamics in complex terrain of semiarid areas: 2. Energy-water controls of vegetation spatiotemporal dynamics and topographic niches of favorability. *Water Resources Research*, *44*(3), W03430. https://doi.org/10.1029/2006WR005595

Jeffery, M. L., Yanites, B. J., Poulsen, C. J., & Ehlers, T. A. (2014). Vegetation-precipitation controls on Central Andean topography. *Journal of Geophysical Research: Earth Surface*, 2013JF002919. https://doi.org/10.1002/2013JF002919

Karl, T. R., & Knight, R. W. (1998). Secular trends of precipitation amount, frequency, and intensity in the United States. *Bulletin of the American Meteorological Society*, *79*(2), 231–241. https://doi.org/10.1175/1520-0477(1998)079<0231:STOPAF>2.0.CO;2

Kharin, V. V., Zwiers, F. W., Xuebin Zhang, & Hegerl, G. C. (2007). Changes in Temperature and Precipitation Extremes in the IPCC Ensemble of Global Coupled Model Simulations. *Journal of Climate*, *20*(8), 1419–1444. https://doi.org/10.1175/JCLI4066.1

Klepper, E. L., Gano, K. A., & Cadwell, L. L. (1985). *Rooting Depth and Distributions of Deep-Rooted Plants in the 200 Area Control Zone of the Hanford Site* (No. PNL-5247). Pacific Northwest Lab., Richland, WA (USA). Retrieved from https://www.osti.gov/scitech/biblio/5989476

Knapp, A. K., Fay, P. A., Blair, J. M., Collins, S. L., Smith, M. D., Carlisle, J. D., … McCarron, J. K. (2002). Rainfall Variability, Carbon Cycling, and Plant Species Diversity in a Mesic Grassland. *Science*, *298*(5601), 2202–2205. https://doi.org/10.1126/science.1076347

Knapp, A. K., Beier, C., Briske, D. D., Classen, A. T., Luo, Y., Reichstein, M., … Weng, E. (2008). Consequences of More Extreme Precipitation Regimes for Terrestrial Ecosystems. *BioScience*, *58*(9), 811. https://doi.org/10.1641/B580908

Kuruppuarachchi, T., & Wyrwoll, K.-H. (1992). The role of vegetation clearing in the mass failure of hillslopes: Moresby Ranges, Western Australia. *CATENA*, *19*(2), 193–208. https://doi.org/10.1016/0341-8162(92)90024-6

Laio, F., Porporato, A., Ridolfi, L., & Rodriguez-Iturbe, I. (2001). Plants in water-controlled ecosystems: active role in hydrologic processes and response to water stress: II. Probabilistic soil moisture dynamics. *Advances in Water Resources*, *24*(7), 707–723. https://doi.org/10.1016/S0309-1708(01)00005-7

Lebourgeois, F., Mérian, P., Courdier, F., Ladier, J., & Dreyfus, P. (2012). Instability of climate signal in tree-ring width in Mediterranean mountains: a multi-species analysis. *Trees*, *26*(3), 715–729. https://doi.org/10.1007/s00468-011-0638-7

Loughridge, R. (2014). Identifying Topographic Controls of Terrestrial Vegetation Using Remote Sensing Data in a Semiarid Mountain Watershed, Idaho, USA. *Boise State University Theses and Dissertations*. Retrieved from http://scholarworks.boisestate.edu/td/888

Ma, X., Huete, A., Moran, S., Ponce-Campos, G., & Eamus, D. (2015). Abrupt shifts in phenology and vegetation productivity under climate extremes: Ecosystem functional response to drought. *Journal of Geophysical Research: Biogeosciences*. https://doi.org/10.1002/2015JG003144

Macias, M., Andreu, L., Bosch, O., Camarero, J. J., & Gutiérrez, E. (2006). Increasing Aridity is Enhancing Silver Fir Abies Alba Mill.) Water Stress in its South-Western Distribution Limit. *Climatic Change*, *79*(3–4), 289–313. https://doi.org/10.1007/s10584-006-9071-0

Malanson, G. P., Butler, D. R., Fagre, D. B., Walsh, S. J., Tomback, D. F., Daniels, L. D., … Millar, C. I. (2007). Alpine Treeline of Western North America: Linking Organism-To-Landscape Dynamics. *Physical Geography*, *28*(5), 378–396. https://doi.org/10.2747/0272-3646.28.5.378

Manfreda, S., & Caylor, K. K. (2013). On the Vulnerability of Water Limited Ecosystems to Climate Change. *Water*, *5*(2), 819–833. https://doi.org/10.3390/w5020819

McAuliffe, J. R., McFadden, L. D., Roberts, L. M., Wawrzyniec, T. F., Scuderi, L. A., Meyer, G. A., & King, M. P. (2014). Non-equilibrium hillslope dynamics and irreversible landscape changes at a shifting pinyon–juniper woodland ecotone. *Global and Planetary Change*, *122*, 1–13. https://doi.org/10.1016/j.gloplacha.2014.07.008

McNamara, J. (1999). *Continuous monitoring in the Dry Creek Experimental Watershed*. Hydrologic Sciences, Dept of Geoscience, Boise State University, Boise, ID.

Moss, R., Babiker, M., Brinkman, S., Calvo, E., Carter, T., Edmonds, J., … Zurek, M. (2008). *Towards New Scenarios for Analysis of Emissions, Climate Change, Impacts, and Response Strategies* (p. 132). Geneva: Intergovernmental Panel on Climate Change.

O'Loughlin, C. L. (1974). The effect of timber removal on the stability of forest soils. *Journal of Hydrology (NZ), 13*(2), 121–134.

Paschalis, A., Katul, G. G., Fatichi, S., Manoli, G., & Molnar, P. (2016). Matching ecohydrological processes and scales of banded vegetation patterns in semiarid catchments. *Water Resources Research, 52*(3), 2259–2278. https://doi.org/10.1002/2015WR017679

Porporato, A., Laio, F., Ridolfi, L., & Rodriguez-Iturbe, I. (2001). Plants in water-controlled ecosystems: active role in hydrologic processes and response to water stress: III. Vegetation water stress. *Advances in Water Resources*, *24*(7), 725–744. https://doi.org/10.1016/S0309-1708(01)00006-9

Poulos, M. J., Pierce, J. L., Flores, A. N., & Benner, S. G. (2012). Hillslope asymmetry maps reveal widespread, multi-scale organization: MAPPING HILLSLOPE ASYMMETRY. *Geophysical Research Letters*, *39*(6), n/a-n/a. https://doi.org/10.1029/2012GL051283

Renwick, K. M., & Rocca, M. E. (2015). Temporal context affects the observed rate of climate-driven range shifts in tree species: Importance of temporal context in tree range shifts. *Global Ecology and Biogeography*, *24*(1), 44–51. https://doi.org/10.1111/geb.12240

Riestenberg, M. M., & Sovonick-Dunford, S. (1983). The role of woody vegetation in stabilizing slopes in the Cincinnati area, Ohio. *Geological Society of America Bulletin*, *94*(4), 506–518. https://doi.org/10.1130/0016-7606(1983)94<506:TROWVI>2.0.CO;2

Rodriguez-Iturbe, I. (2000). Ecohydrology: A hydrologic perspective of climate-soil-vegetation dynamies. *Water Resources Research*, *36*(1), 3–9. https://doi.org/10.1029/1999WR900210

Roering, J. J., Schmidt, K. M., Stock, J. D., Dietrich, W. E., & Montgomery, D. R. (2003). Shallow landsliding, root reinforcement, and the spatial distribution of trees in the Oregon Coast Range. *Canadian Geotechnical Journal*, *40*(2), 237–253. https://doi.org/10.1139/t02-113

Rossi, S., Deslauriers, A., Griçar, J., Seo, J.-W., Rathgeber, C. B., Anfodillo, T., … Jalkanen, R. (2008). Critical temperature for xylogenesis in conifers of cold climates. *ResearchGate*, *17*(6), 696–707. https://doi.org/10.1111/j.1466-8238.2008.00417.x

Rupp, D. E., Abatzoglou, J. T., Hegewisch, K. C., & Mote, P. W. (2013). Evaluation of CMIP5 20th century climate simulations for the Pacific Northwest USA. *Journal of Geophysical Research: Atmospheres*, *118*(19), 2013JD020085. https://doi.org/10.1002/jgrd.50843

Schimel, D. S. (2010). Drylands in the Earth System. *Science*, *327*(5964), 418–419. https://doi.org/10.1126/science.1184946

Schmidt, K. M., Roering, J. J., Stock, J. D., Dietrich, W. E., Montgomery, D. R., & Schaub, T. (2001). The variability of root cohesion as an influence on shallow landslide susceptibility in the Oregon Coast Range. *Canadian Geotechnical Journal*, *38*(5), 995–1024.

Schwinning, S., Starr, B. I., & Ehleringer, J. R. (2005a). Summer and winter drought in a cold desert ecosystem (Colorado Plateau) part I: effects on soil water and plant water uptake. *Journal of Arid Environments*, *60*(4), 547–566. https://doi.org/10.1016/j.jaridenv.2004.07.003

Schwinning, S., Starr, B. I., & Ehleringer, J. R. (2005b). Summer and winter drought in a cold desert ecosystem (Colorado Plateau) part II: effects on plant carbon assimilation and growth. *Journal of Arid Environments*, *61*(1), 61–78. https://doi.org/10.1016/j.jaridenv.2004.07.013

Sillmann, J., Kharin, V. V., Zhang, X., Zwiers, F. W., & Bronaugh, D. (2013). Climate extremes indices in the CMIP5 multimodel ensemble: Part 1. Model evaluation in

the present climate. *Journal of Geophysical Research: Atmospheres*, *118*(4), 1716–1733. https://doi.org/10.1002/jgrd.50203

Smith, T. J., McNamara, J. P., Flores, A. N., Gribb, M. M., Aishlin, P. S., & Benner, S. G. (2011). Small soil storage capacity limits benefit of winter snowpack to upland vegetation: Limited soil storage constrains snowpack benefits. *Hydrological Processes*, *25*(25), 3858–3865. https://doi.org/10.1002/hyp.8340

Suarez, M. L., Villalba, R., Mundo, I. A., & Schroeder, N. (2015). Sensitivity of Nothofagus dombeyi tree growth to climate changes along a precipitation gradient in northern Patagonia, Argentina. *Trees*, *29*(4), 1053–1067. https://doi.org/10.1007/s00468-015-1184-5

Sun, Y., Solomon, S., Dai, A., & Portmann, R. W. (2007). How Often Will It Rain? *Journal of Climate*, *20*(19), 4801–4818. https://doi.org/10.1175/JCLI4263.1

Swetnam, T. W., & Betancourt, J. L. (1998). Mesoscale Disturbance and Ecological Response to Decadal Climatic Variability in the American Southwest. *Journal of Climate*, *11*(12), 3128–3147. https://doi.org/10.1175/1520-0442(1998)011<3128:MDAERT>2.0.CO;2

Tabler, R. D. (1964). The Root System of Artemisia Tridentata at 9,500 Feet in Wyoming. *Ecology*, *45*(3), 633–636. https://doi.org/10.2307/1936115a

Terwilliger, V. J., & Waldron, L. J. (1991). Effects of root reinforcement on soil-slip patterns in the Transverse Ranges of southern California. *Geological Society of America Bulletin*, *103*(6), 775–785. https://doi.org/10.1130/0016-7606(1991)103<0775:EORROS>2.3.CO;2

Tesfa, T. K., Tarboton, D. G., Chandler, D. G., & McNamara, J. P. (2009). Modeling soil depth from topographic and land cover attributes. *Water Resources Research*, *45*(10). https://doi.org/10.1029/2008WR007474

Thompson, S. E., Katul, G. G., & Porporato, A. (2010). Role of microtopography in rainfall-runoff partitioning: An analysis using idealized geometry. *Water Resources Research*, *46*(7), W07520. https://doi.org/10.1029/2009WR008835

Tucker, G. (2013). The ModelGrid Package.

Tucker, G. E., & Bras, R. L. (1998). Hillslope processes, drainage density, and landscape morphology. *Water Resources Research, 34*(10), 2751–2764. https://doi.org/10.1029/98WR01474

Tucker, G. E., Hobley, D. E. J., Hutton, E., Gasparini, N. M., Istanbulluoglu, E., Adams, J. M., & Nudurupati, S. S. (2016). CellLab-CTS 2015: continuous-time stochastic cellular automaton modeling using Landlab. *Geoscientific Model Development, 9*(2), 823–839. https://doi.org/10.5194/gmd-9-823-2016

Tucker, G. E., Lancaster, S. T., Gasparini, N. M., Bras, R. L., & Rybarczyk, S. M. (2001). An object-oriented framework for distributed hydrologic and geomorphic modeling using triangulated irregular networks. *Computers & Geosciences*, *27*(8), 959–973.

Villalba, R., & Veblen, T. T. (1998). Influences of Large-Scale Climatic Variability on Episodic Tree Mortality in Northern Patagonia. *Ecology*, *79*(8), 2624–2640. https://doi.org/10.1890/0012-9658(1998)079[2624:IOLSCV]2.0.CO;2

Vivoni, E. R., Rinehart, A. J., Méndez-Barroso, L. A., Aragón, C. A., Bisht, G., Cardenas, M. B., … Wyckoff, R. L. (2008). Vegetation controls on soil moisture distribution in the Valles Caldera, New Mexico, during the North American monsoon. *Ecohydrology*, *1*(3), 225–238. https://doi.org/10.1002/eco.11

Wilcox, B. P., Turnbull, L., Young, M. H., Williams, C. J., Ravi, S., Seyfried, M. S., … Wainwright, J. (2012). Invasion of shrublands by exotic grasses: ecohydrological consequences in cold versus warm deserts. *Ecohydrology*, *5*(2), 160–173. https://doi.org/10.1002/eco.247

Williams, A. P., Allen, C. D., Macalady, A. K., Griffin, D., Woodhouse, C. A., Meko, D. M., … McDowell, N. G. (2012). Temperature as a potent driver of regional forest drought stress and tree mortality. *Nature Climate Change*, *3*(3), nclimate1693. https://doi.org/10.1038/nclimate1693

Wu, T. H., McKinnell III, W. P., & Swanston, D. N. (1979). Strength of tree roots and landslides on Prince of Wales Island, Alaska. *Canadian Geotechnical Journal*, *16*(1), 19–33. https://doi.org/10.1139/t79-003

Yetemen, O., Istanbulluoglu, E., Flores-Cervantes, J. H., Vivoni, E. R., & Bras, R. L. (2015). Ecohydrologic role of solar radiation on landscape evolution. *Water Resources Research*, n/a-n/a. https://doi.org/10.1002/2014WR016169

Yetemen, O., Istanbulluoglu, E., & Vivoni, E. R. (2010). The implications of geology, soils, and vegetation on landscape morphology: Inferences from semi-arid basins with complex vegetation patterns in Central New Mexico, USA. *Geomorphology*, *116*(3–4), 246–263. https://doi.org/10.1016/j.geomorph.2009.11.026

Zhang, X., Zwiers, F. W., Hegerl, G. C., Lambert, F. H., Gillett, N. P., Solomon, S., … Nozawa, T. (2007). Detection of human influence on twentieth-century precipitation trends. *Nature*, *448*(7152), 461–465. https://doi.org/10.1038/nature06025

Zhou, X., Istanbulluoglu, E., & Vivoni, E. R. (2013). Modeling the ecohydrological role of aspect-controlled radiation on tree-grass-shrub coexistence in a semiarid climate. *Water Resources Research*, *49*(5), 2872–2895. https://doi.org/10.1002/wrcr.20259

Zotarelli, L., Dukes, M. D., Romero, C. C., Migliaccio, K. W., & Morgan, K. T. (2010). Step by step calculation of the Penman-Monteith Evapotranspiration (FAO-56 Method). *Institute of Food and Agricultural Sciences. University of Florida*. Retrieved from http://storm.okstate.edu/bae3313/fall%202013/lecture/5)%20ET/Penman-Monteith.pdf

APPENDIX A

Where to Find Our Code

Our code can be found at https://github.com/LEAF-BoiseState/SWIdahoLandlab. The ‘CA_veg’ directory contains the code used to model vegetation. The ‘PFT_stats’ directory contains code used to analyze and visualize the output of the vegetation model. The ‘PrecipitationStatisticsCode’ directory contains both the historical DCEW meteorological data and the code used to distil descriptive statistics of that data. We determined how many replicates to run and for how long using the code in the ‘ReplicateSensitivityAnalysis’ directory. Finally, we created our synthetic DEM with the code in the ‘erosion_driver’ directory. All code is written in Python, except the sensitivity analysis of replicates, which is in MATLAB.

APPENDIX B

Creation of Synthetic DEM Using Landlab

We created a synthetic DEM to use as the topographic input for our climate scenarios so that we could design the topography to exaggerate the microclimates we were most interested in studying. Primarily, we wanted to examine the differences between north- and south-facing aspects, aspect being a strong driver of solar and thus soil moisture variation (Burnett, Meyer, & McFadden, 2008), so we designed our DEM to have slopes predominantly facing in those directions. The effects of aspect on vegetation is due to differences in radiation received (Anderson et al., 2014), so we also designed our DEM to have a slope curvature that matched the curvature of hillslopes in DCEW, the semi-arid watershed our weather scenarios were based upon.

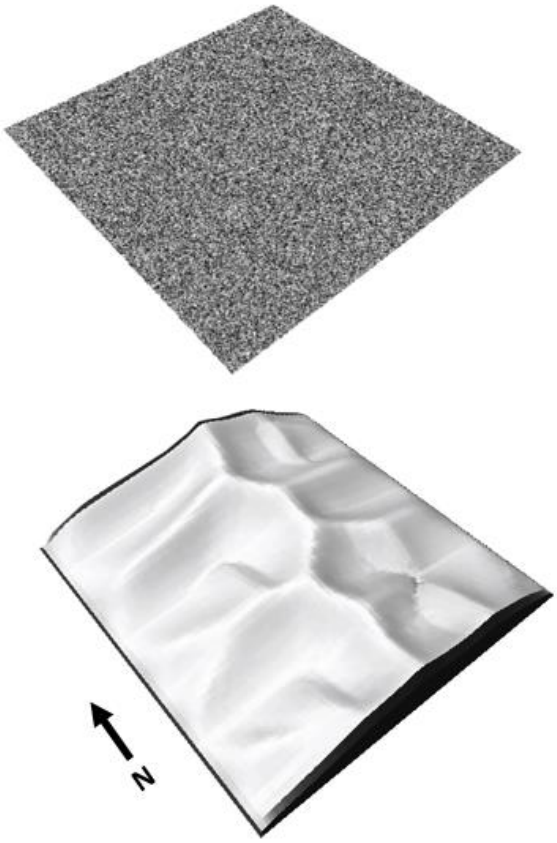

Figure B.18: Isometric View of Initial Flat Topography with "Noise" (Top) and Final Extruded Topography.

In creating our DEM, we did not evaluate elevation change. In our model the entire DEM, regardless of elevation, received the same weather, making the difference of null importance. Instead, we ran a sensitivity test of the vegetation in our model to the precipitation at different weather stations along an elevation gradient (Appendix D). There were significant differences between the simulated vegetation at these different elevations. We chose to create our climate scenarios from the weather station closest to the ecotone, where vegetation is most at risk of alteration due to climate change (Allen & Breshears, 1998).

Finally, by running our model on a synthetic DEM we removed any impacts of DCEW on the specific microclimates. We can safely conclude that the findings of our study will be applicable to any site with a similar landscape, ecosystem, and climate, instead of confining the applicability to just a single area.

Methods: Creation of DEM

Landlab erodes the landscape by moving sediment downhill and then off the edge of the grid (see Tucker, 2013). This necessitates an initial grid that is not flat, so sediment has somewhere to move towards. We created a 100 by 100 node grid and populated that grid with topographic noise (Figure B.18). Each node can be translated into a 1 by 1 m pixel.

We wanted to create a landscape whose hillslopes faced mostly north and south, so we created a ridge running north-south for all the subsequent smaller watersheds to flow from. The main sides of the watersheds are perpendicular to the direction of flow, which is away from the main ridge, or east-west (Figure B.20). We did this by restricting the boundaries that sediment could flow out of to only the east and west edges.

We ran the model for 100 years to create topography with similar hillslope curvature to DCEW (measured with ArcMap using a Lidar-derived DEM). To do this we used three modules: linear diffusion, stream power eroder, and the flow router that the stream power eroder relies on. We also uplifted the topography at every time step.

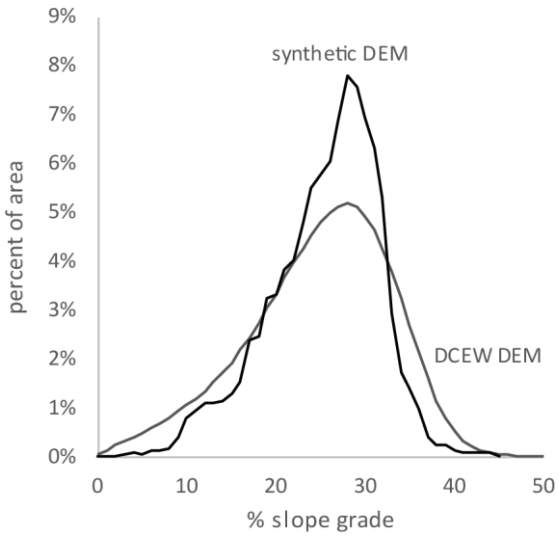

Figure B.19: Distribution of Slopes in Our Synthetic DEM as Compared with the Topography in DCEW. Slope Angles in the Synthetic DEM Cluster More Closely Around the Mean, While the Natural Topography Has More Slopes at the Shallow and Steep Ends of the Continuum. Overall, Though, the Distributions Cluster Around the Same Mean of High 20s for Their Grade.

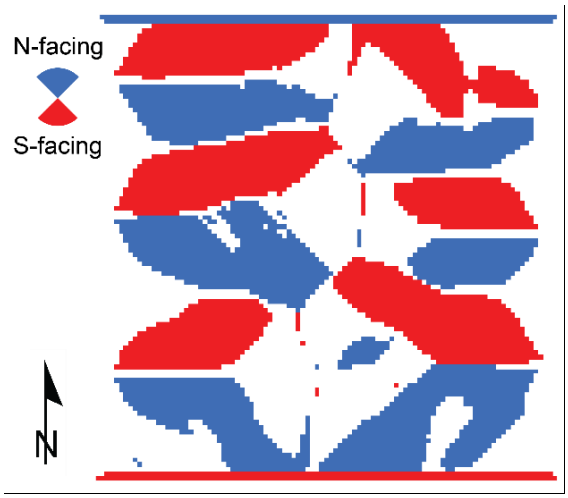

Figure B.20: Map of the Distribution of North- and South-facing Hillslopes Within the Synthetic DEM. The North to South Running Ridgeline in the Center of the Image Is Flat on Top, and Then Shifts to East- (on the Right Side of the Figure) or West-facing (on the Left Side) at the Top of Their Respective Watersheds. This Area is Shaded White

Table B.8: Forcings Used to Create the Topography We Used for Our Vegetation Modelling.

Uplift rate	Erodi-bility	M sp	N sp	rock density	sediment density	sediment erosivity	S crit	linear diffusivity
0.01	0.3	0.5	1	2.7	2.7	0.0001	0.56	0.0005

REFERENCES

Allen, C. D., & Breshears, D. D. (1998). Drought-induced shift of a forest–woodland ecotone: Rapid landscape response to climate variation. Proceedings of the National Academy of Sciences, 95(25), 14839–14842.

Anderson, B. T., McNamara, J. P., Marshall, H.-P., & Flores, A. N. (2014). Insights into the physical processes controlling correlations between snow distribution and terrain properties. *Water Resources Research*, *50*(6), 4545–4563. https://doi.org/10.1002/2013WR013714

Burnett, B. N., Meyer, G. A., & McFadden, L. D. (2008). Aspect-related microclimatic influences on slope forms and processes, northeastern Arizona. *Journal of Geophysical Research: Earth Surface*, *113*(F3), F03002. https://doi.org/10.1029/2007JF000789

Tucker, G. (2013). The ModelGrid Package.

APPENDIX C

Generation of Storms Within Landlab

Landlab's stochastic storm generator uses three forcings to create weather: storm length, inter-storm length, and precipitation depth per storm. The storm generator generates a Poisson distribution based on each of these (Laio et al., 2001), and the values in the Poisson distribution create the variety of weather the model uses. These values are critical, as they define the water available for the growth of plants. There are two different seasons in our model, wet, and dry. Both seasons have their own base storm component forcings, which we determined using data from precipitation gauges at Treeline Weather Station, located with DCEW (McNamara, 1999).

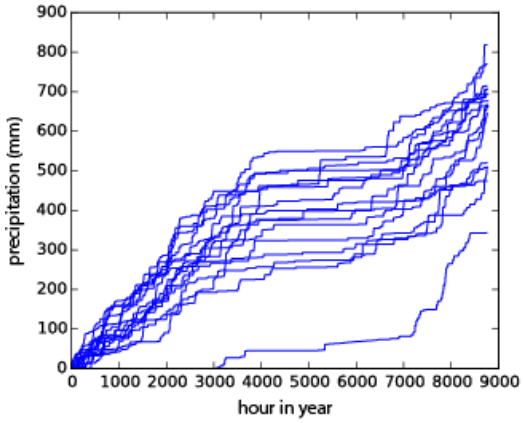

Figure C.21: Precipitation Received at Treeline Gauge in DCEW, From 1999-2014. The Lines Level Off in the Middle of the Year, Where Summer Precipitation is Low. The Bottom Line That Starts at Hour 3000 Is From the First Year the Gauge Was Installed.

It is important that we make the distinction between wet and dry season, as precipitation distribution is temporally stratified in this region (Figure C.21, Figure C.22; C. Hanson & Johnson, 2001). Though distribution of storm depths is around the same in both the wet and the dry seasons (Figure C.22), inter-storm duration is greater in dry seasons than in wet ones (Figure C.23). A minority of inter-storm instances make up the long tail of the dry season's distribution of inter-storm instances, but those occurrences

by definition have an outsized impact, and drive the discrepancy between total precipitation in dry and wet seasons. After examining the available data from Treeline, we defined the wet season as Julian day 0 through 171 and 270 through 365, and the dry season as days 171 through 270.

The precipitation gauges take measurements in millimeters to two decimal points on an hourly basis. We defined a storm event as having occurred when precipitation exceeded 1.00 mm for one hour, a depth which is significant at a location that only receives 656 mm of rainfall per year (Aishlin & McNamara, 2011).

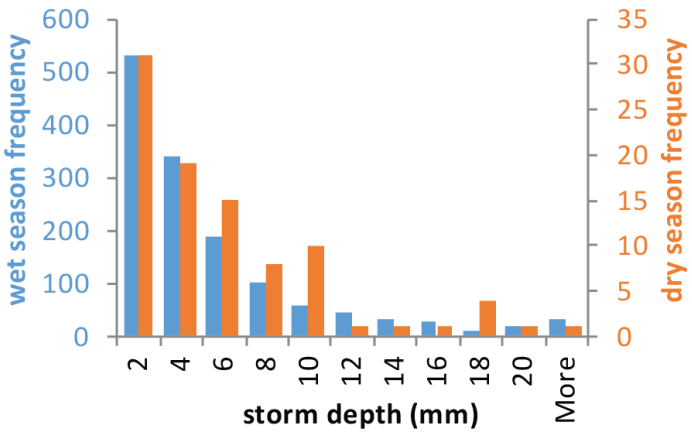

Figure C.22: Frequency Distribution of Total Water Received During Each Storm (Storm Depth).

We counted any consecutive hour for which the rainfall depth exceeded 1 mm as a single storm event, adding all rainfall together to determine the total depth of storm precipitation over a storm event (Figure C.22) and all hours together to determine the length of that storm (Figure C.23, left). Inter-storm length was defined as all consecutive hours that received less than 1 mm of precipitation each (Figure C.23, right). Thus, both

inter-storm and storm length was measured in hours, and storm depth was measured in total mm accumulated.

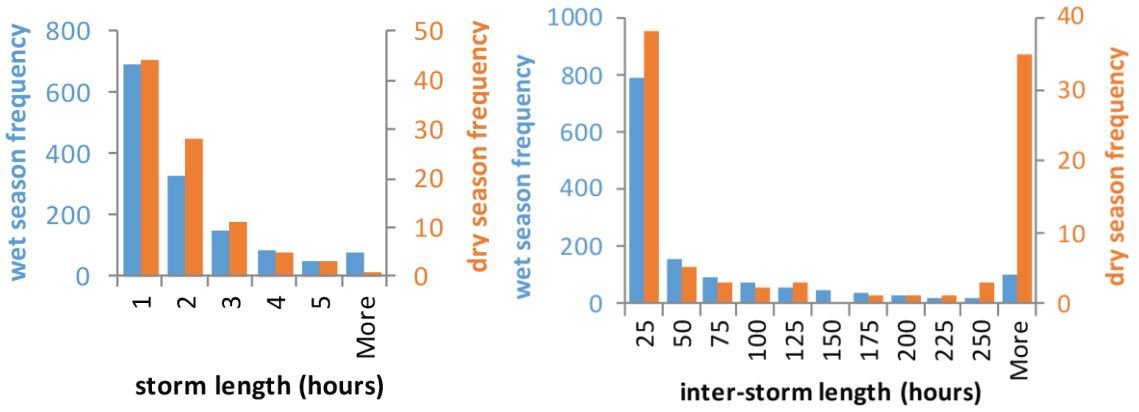

Figure C.23: Frequency Distribution of Length of Storms (Left) and Length of Inter-Storm Duration (Right) Measured at Treeline in DCEW in Hours

In general, the distribution of all the statistics describing storm parameters is logarithmic (Figure C.22, Figure C.23). There are far more storms that occur in the wet season than do in the dry season, but the overall pattern is the same, if not the magnitude. Storm lengths mostly fall between one and five hours, while the inter-storm length is far more variable, and (especially in the dry season) exhibits a long tail. When it does rain at Treeline, 90% of storms receive rainfall totaling under 10 mm.

REFERENCES

Aishlin, P., & McNamara, J. P. (2011). Bedrock infiltration and mountain block recharge accounting using chloride mass balance. Hydrological Processes, 25(12), 1934–1948. https://doi.org/10.1002/hyp.7950

Hanson, C., & Johnson, G. (2001). Spatial and Temporal Precipitation Characteristics in Southwest Idaho.

Laio, F., Porporato, A., Ridolfi, L., & Rodriguez-Iturbe, I. (2001). Plants in water-controlled ecosystems: active role in hydrologic processes and response to water stress: II. Probabilistic soil moisture dynamics. *Advances in Water Resources*, *24*(7), 707–723. https://doi.org/10.1016/S0309-1708(01)00005-7

McNamara, J. (1999). *Continuous monitoring in the Dry Creek Experimental Watershed*. Hydrologic Sciences, Dept of Geoscience, Boise State University, Boise, ID.

APPENDIX D

DCEW Vegetation Survey

Introduction

Real ecosystems are inherently dynamic, and seeded with vegetation from previous climate regimes (Gibson & Brown, 1985; Horn, 1974; Pastor & Post, 1986), making any direct comparison of an observed ecosystem with the outputs from a model imperfect at best. However, a comparison between the two can yield useful data, such as documenting the disparity between our model and reality, as well as beginning to quantify the level of disturbance of the ecology within DCEW. In this section, we conducted a survey of the vegetation within DCEW to find the data needed to make those comparisons. We divided the vegetation within DCEW into four plant functional type (PFT) categories (bare ground, grasses, shrubs, and trees) and mapped their distribution. We further subdivided vegetation distribution by aspect, elevation, and distance from weather station to make comparisons on a microclimate scale.

From ground observations of this area, and our knowledge of the ecosystem, we predicted that trees would dominate the upper elevations, supplemented by shrubs with a little grass in between the two. By contrast, we thought the lower elevations would have mostly grasses, with some bare ground and patches of shrubs. We expected middle elevations to be a hybrid of the two, with south-facing slopes more closely resembling the grasses of the lower elevations and north-facing slopes comparable to the trees in the upper elevations. Though some of those predictions were correct, we instead found patterns that were much more complicated, reflecting the impacts of humans and changing climates on the vegetation within DCEW.

Methods: PFT Type Categorization and Mapping

For our modelling, we sorted all plant species into four categories of PFT: tree, shrub, grass, or bare ground. This categorization minimized computational time for Landlab, but did result in the loss of information related to differences between varying species of the same PFT. Throughout this paper, we refer to PFT, or percent PFT. When we do so, we mean the percent of ground cover by area that a given PFT covers. Figure D.24 shows an example of how plant size corresponds to percent PFT.

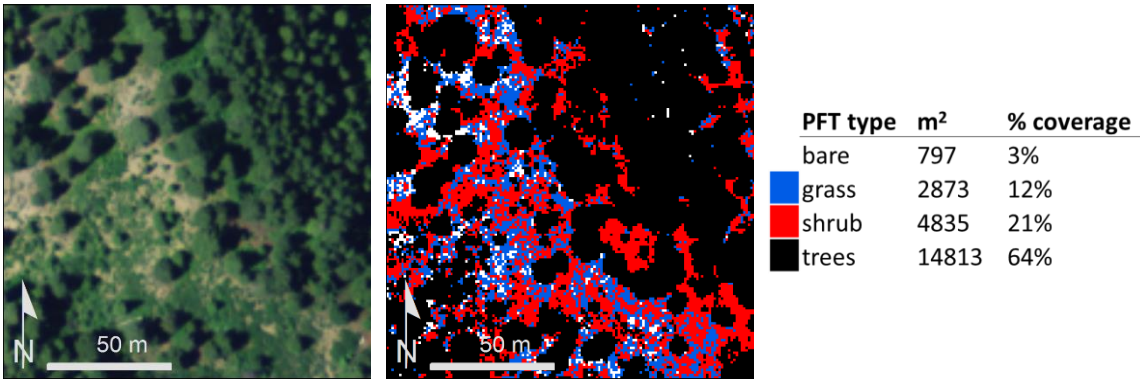

Figure D.24: Example PFT Categorization Workflow. Our Algorithm Classified Tall Vegetation (Dark Green in Left Aerial Photo) as Trees and Colored Them Black in the Middle Map. In the Table on the Right, Trees Cover 14813 m^2, or 64% of the Area.

We wanted to compare the results of our model's climate scenarios to real world vegetation. To do so, we quantified the distribution of vegetation within DCEW using vegetation height as a proxy for PFT type (Donoghue et al., 2007). We used 2007 snow-off LiDAR files generated by the University of Idaho and published by the Idaho LiDAR Consortium to find vegetation height. This data was in LAS file format, and had an average point spacing of a little over 6 points per m^2 (Idaho LiDAR Consortium, 2007).

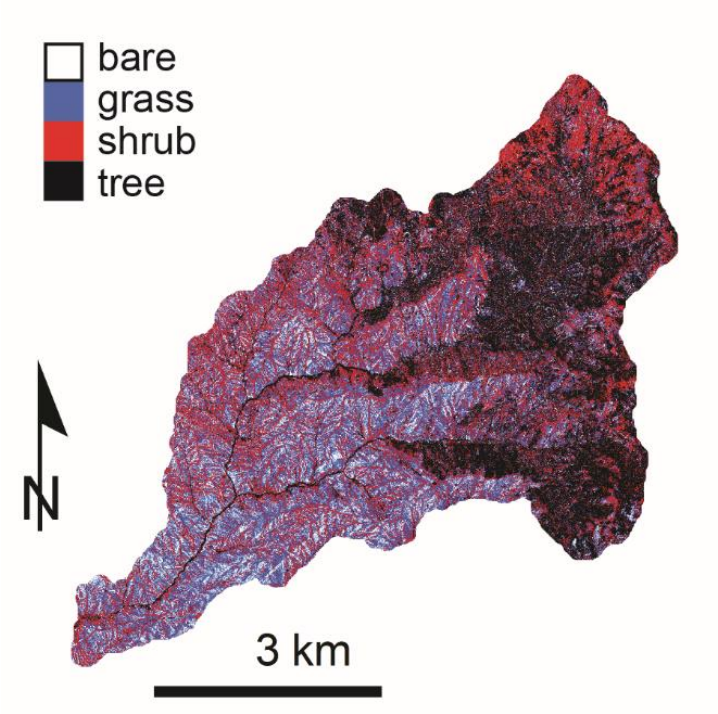

Figure D.25: Distribution of Vegetation Throughout DCEW, by Our Four PFT Classifications

We processed the LiDAR files using BCAL LiDAR tools, generating two 1 m resolution raster files: a DEM of bare ground, and a raster of first returns showing canopy elevation. We determined vegetation height by subtracting bare ground elevation from the canopy returns. Using this vegetation height, we classified all vegetation into four different categories and generated a raster mapping this distribution. The height categories for the four PFT categories were as follows: 0.15-0.5 m for grasses, 0.5-1.5 m for the shrubs, and over 1.5 m for the trees. This classification yielded a 1 m raster map of vegetation type throughout DCEW (Figure D.25). In order to compare the percent PFT distribution found in our model outputs to real DCEW data, we needed to subdivide the DCEW vegetation map so that vegetation cover could be associated with each weather station. We subdivided the vegetation within ArcMap using two strategies: by using

elevation bins associated with each weather stations and by using circular buffers of varying sizes around each weather station. Both strategies identified percent PFT by aspect for each weather station, but the techniques used were different; they each have a section detailing their respective methods.

Methods: Identification of Percent PFT by Elevation

For our elevation-determined analysis, we divided the watershed's vegetation into 10 sections, each representing 100 meters of elevation (Figure D.26) using the Contour tool. Our model does not account for riparian vegetation, so we removed vegetation within 25 m of streams. First, we delineated the rivers using a DEM (with the tools Fill, Aspect, Flow Direction, Flow Accumulation, and Classify). We chose our flow accumulation number by observing aerial photos and determining the areas where riparian trees were growing (see Figure D.27). We then Buffered these streams, used Polygon to Raster to convert the shapefile into a raster, and inverted that raster to only include areas that did not have the stream buffer (the transparent white layer in Figure D.27). With this step complete, we were able to use the Raster Calculator to create rasters that contained only vegetation from outside the buffer area, on a single aspect, within the target elevation band. Equation 1 shows an example of the equation used within Raster Calculator. For this example, we found vegetation on north-facing aspects, between 1070 and 1170 m, on areas where there are no river buffers.

```
Con(("DCEW_rivers" == 0) &                                                    (1)
    ("DCEW_DEM" > 1070) & ("DCEW_DEM" < 1170) &
    ("DCEW_aspect" < 45) | ("DCEW_aspect" > 315) , "DCEW_4class_veg")
```

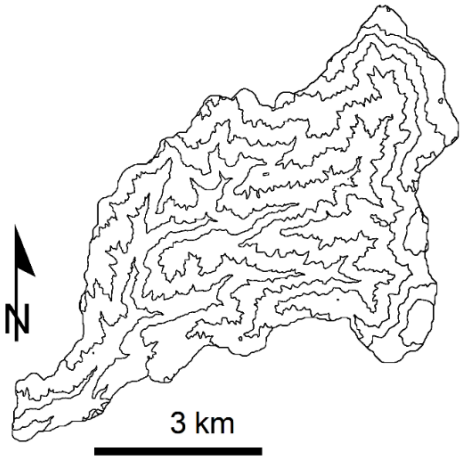

Figure D.26: Contour Lines Depicting How We Subdivided DCEW Into 10 Sections by Elevation

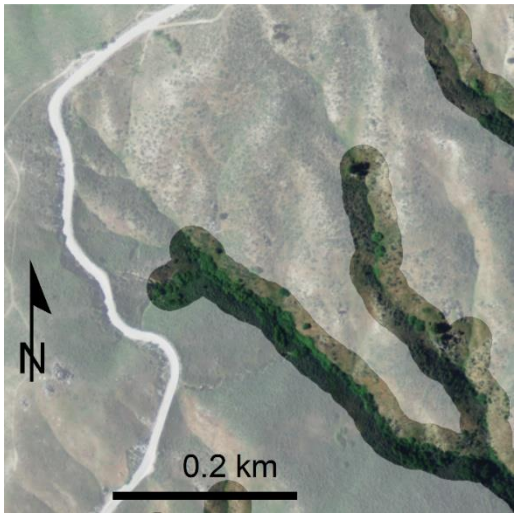

Figure D.27: Aerial Photo Showing Buffer of 25 m Around Each Stream. We Chose Stream Lengths Through Trial and Error by Viewing Aerial Photos Such as the One Shown Here.

Methods: Identification of Percent PFT by Weather Station Buffers

We used a python script to create weather station buffers. We imported a DEM and used the Aspect tool to find the north and south facing hillslopes in DCEW. We used this hillslope and a conditional formula similar to that in the previous section to create separate rasters of vegetation on the two facing hillslopes. We then imported a pointfile of the weather stations and buffered those stations. We chose four different buffer sizes: 250 m, 500 m, 750 m, and 1 km (Figure D.28). To use the raster calculator, we then converted these buffer polygons to rasters, using the Polygon to Raster tool.

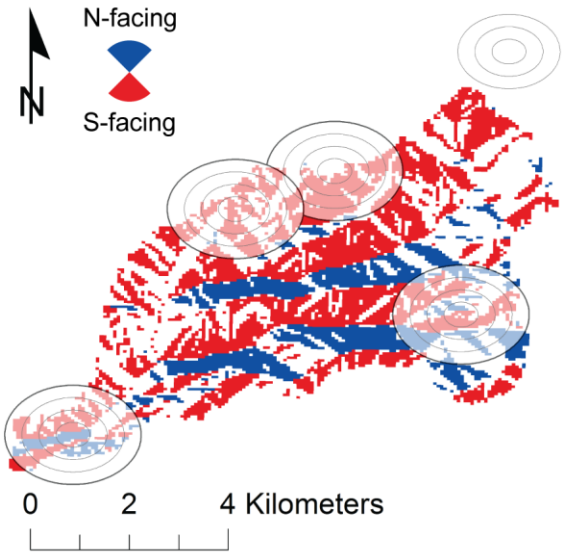

Figure D.28: Four Different Buffers Around the Weather Stations Located Within DCEW, Against a Map of Hillslope Aspect

Once the buffer and vegetation rasters were in place, we used a for-loop to evaluate the percent PFT coverage for each weather station by hillslope. Looping through each of the stations in turn, we created temporary rasters with Raster Calculator and then wrote those attribute files to a .csv file created outside of the for-loop.

Results

At lower elevations, grass and shrubs predominate (totaling about 80% area coverage,Figure D.29) with almost no trees (1%). As higher elevations, there start to be more trees, which push out grasses (about 50% and 15% respectively across the upper elevations). Shrubs stay about the same percent coverage (around 30%) for all elevations except 1800 m and 1900 m. At those two elevations, shrubs increase to 41% and 58% reflectively and there is less tree coverage to make room for these extra trees. There is the most bare ground at the lowest elevation (22%), and that steadily decreases in the upper elevations to about 6%. Grasses follow a similar pattern; they start at 49% ground cover and decrease to 13%.

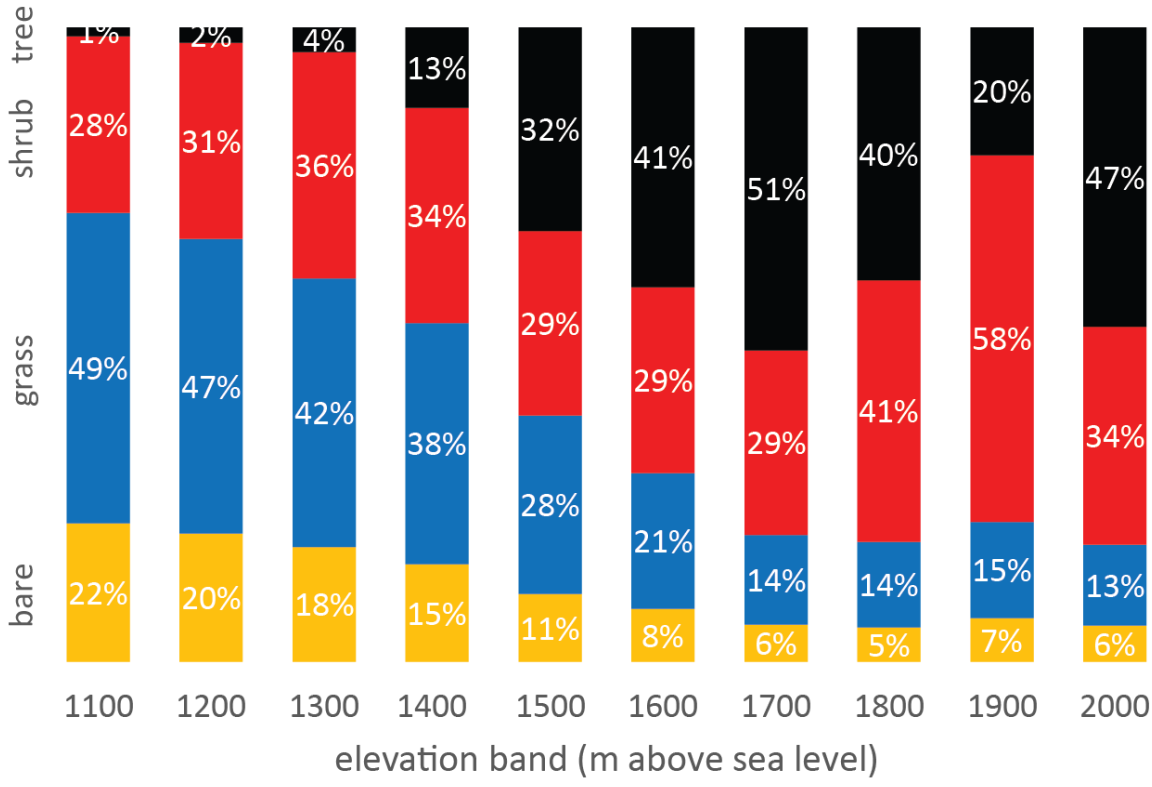

Figure D.29: Distribution of Vegetation Throughout the Watershed, by PFT and Elevation Band.

We chose to focus on DCEW's Treeline weather station for a more in-depth analysis (Figure D.30). This weather station is located at the elevation of the current tree-line, where vegetation changes from the sagebrush (Artemisea tridentate), grasses, and bitterbrush (Prushia tridentata) characteristic of lower elevations to the Ponderosa Pine (Pinus ponderosa), Douglas Fir (Pseudotsuga menziesii), and Green Alder (Alnus viridis) trees that are predominant higher in the watershed (Anderson et al., 2014). For this comparison, we used our model to simulate what the vegetation would be like using the current weather. We completed this comparison twice, once adjusted to the downscaling from RCP 4.5, and again adjusted to RCP 8.5 ((IPCC) Intergovernmental Panel on Climate Change, 2007). Though the forecasts themselves were different, since we are using contemporary weather for this model they should show similar weather patterns. Both forecasts were included to account for the effects of downscaling, and comparing them against one another allowed for another check. The results for the two were similar, as expected; none of the numbers for percent PFT coverage were different between the two models by more than 1%.

The buffer following a contour line equal with the elevation of Treeline weather station (1560 m) was the closest to Landlab's modelled climate scenarios (RCP 4.5 and 8.5). For the south-facing slope of the contour buffer, the modelled vegetation was off by 6% or less. However, the 1560 m north-facing slopes deviate sharply. There is only 24% tree cover on the contour, to the model's 55%. Shrubbery on this aspect is still within 5% of the models, but grasses expanded to cover 33% of the contour's ground, up three times from the model's 11%. Bare ground almost doubled within the contour, from 7% to 13%, although that is still less than a 6% change.

The two circular buffers around Treeline weather station differed more greatly from the model's outputs than the elevation contour. Tree coverage shrunk, to 3-39% for the 1000 m and 750 m buffers (compared to the model's 51-55%). Shrub coverage increased, but only by about 10%. Grasses and bare ground coverage matched that of the north-facing slope within the 1560 elevation buffer. Of these numbers, the north-facing slope within the 1000 m circular buffer matched the model more closely than the other circular buffers, while the south facing 1000 m buffer and north-facing 750 m buffer were the worst.

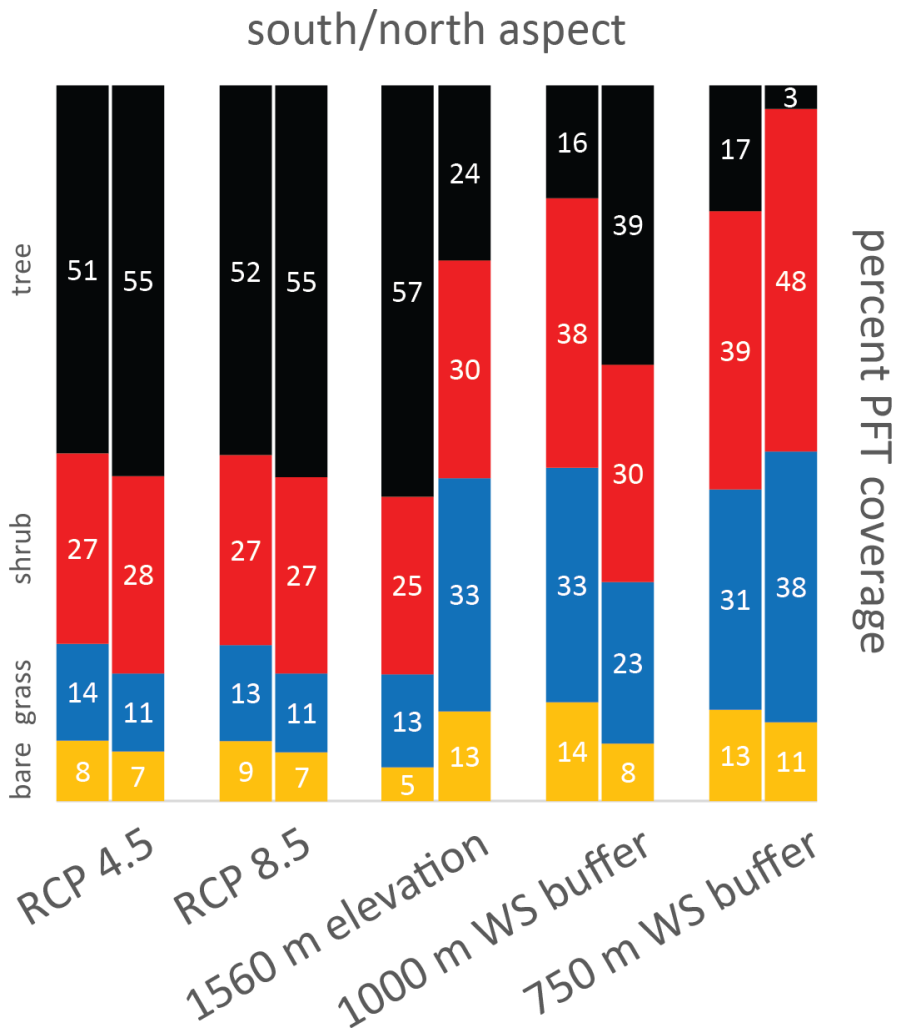

Figure D.30: Percent of Each PFT Located at Treeline Weather Station, As Defined by Two Different Climate Scenarios Run on Landlab As Well As Three Different Buffers Around the Real Weather Station Located Within DCEW. The Percent PFT Shown for the Model Runs Is the Mean of 500 Replicates. The Left Column for Each Is the South Aspect, While the Right Is the North

Discussion

Except for the top three elevation categories (1800-2000), the vegetation within the elevation bands followed the pattern we expected. Trees covered less ground lower in the watershed (1%), and progressively increased in the upper elevations (to 51%). Conversely, grasses and bare ground started out covering 49% and 22% of the ground

respectively and decreased to 13% and 6% respectively. Shrubs remained stable around 30% throughout. However, the top three categories did not follow these trends at all.

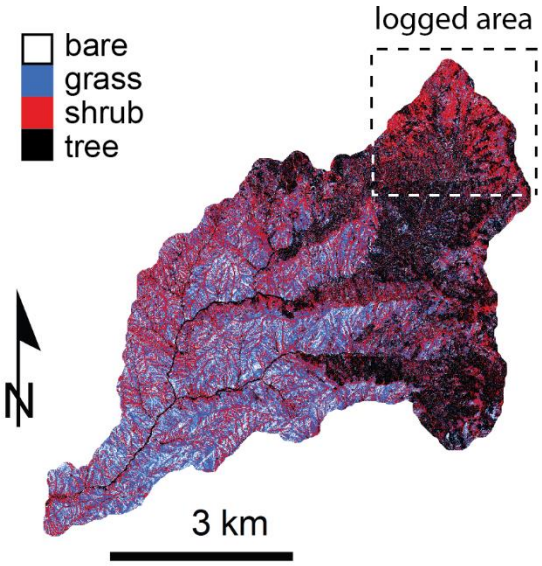

Figure D.31: Within the Dotted Box, a Clear Increase in Shrubs (Red) Is Visible, at the Expense of Trees (Black), along an Unnaturally Straight Line. This Shows Where Logging Likely Took Place

While there could be many natural reasons for this discrepancy, we believe the most logical explanation is logging that took place within the watershed. There are no reliable records of where logging occurred. However, Loughridge (2014) and Anderson et al. (2014) write that the forests in the upper part of the watershed were managed extensively, and there are to this day visual artifacts of this logging still visible in aerial photos (Figure D.32, James McNamara, personal communication, May 2, 2016). The extent of this logging is also visible within our vegetation map created from LiDAR (Figure D.31).

Figure D.32: Close-up of a Section of the Upper Elevation of DCEW. The Dotted Line Follows a Potential Logging Boundary, Not the Effects of a Topographically-induced Microclimate Such as a Ridgeline

Another potential reason for discrepancies between expected patterns and our findings is the large size of the elevation bands (100 m). At the higher elevations, especially around Treeline (at 1560 m elevation), dramatic vegetation changes can take place over much smaller elevational transects than 100 m. Significant changes in soil moisture over a similarly sized elevation transect has been documented (Famiglietti, Rudnicki , & Rodell, 1998). The dissected nature of the watershed could enhance this effect; a north facing hillslope on the east side of the watershed and the top of an elevation band could have an entirely different microclimate than one on the north side at the bottom of the same elevation band.

The north-facing 100 m elevation band associated with the Treeline watershed (1560 m) was different from Landlab's models. In it, tree coverage decreased to 24%, compared to the model's 55%, while grasses expanded dramatically from 11 % to 33% to

fill the empty space. This band was also different from expected by people who have spent time around the weather station (Jen Pierce, personal communication, April 8, 2016). Surprisingly, the south-facing vegetation cover from the same band matches the models closely (with less than 6% difference in all PFT categories). It is possible that this is an example of logging that took place only on certain slopes, perhaps because trees were denser on north-facing hillslopes, and thus were more viable logging targets. There could also be any number of other disturbances taking place as well. Invasives such as Bromus tectorum (cheatgrass) are prevalent within the watershed (Loughridge, 2014). Invasives outcompete native grasses and shrubs, and establish quickly after fires (Bradley et al., 2006). Further, invasives burn more easily than native plants, creating a positive feedback loop that could be altering the native distribution of vegetation (Bradley et al., 2006).

The circular buffers were even more different from the model's predictions than the elevation bands were. All aspects for the two circular buffers had larger grass populations and smaller tree populations than expected. This finding lends more credence to our invasives theory, as B. tectorum would be indistinguishable from the native grasses in our height sorting classification. We confirmed the presence of B. tectorum near these weather stations. This localization of invasives could have overwhelmed the small area within the buffers, skewing the number of trees to be different from the rest of the microclimate.

Conclusion

While some of the 100 m elevation banded vegetation samples were similar to that expected, as well as what the models predicted, at Treeline elevation and above this

strategy broke down. These upper elevations had less trees, breaking the trend of more tree-cover as the survey increased in elevation, and increased shrubs to fill in the gaps. We attribute these missing trees to logging efforts within the upper elevations of DCEW.

The south-facing aspect of the Treeline elevation band was reasonably representative, but the north-facing aspects of that elevation band as well as both circular buffers around Treeline weather station were different from the model's predictions. These samples had fewer trees than the models, and increased grasses to make up the difference. This is likely due to invasive *B. tectorum*.

REFERENCES

Anderson, B. T., McNamara, J. P., Marshall, H.-P., & Flores, A. N. (2014). Insights into the physical processes controlling correlations between snow distribution and terrain properties. *Water Resources Research*, *50*(6), 4545–4563. https://doi.org/10.1002/2013WR013714

Bradley, B. A., Houghton, R. A., Mustard, J. F., & Hamburg, S. P. (2006). Invasive grass reduces aboveground carbon stocks in shrublands of the Western US. *Global Change Biology*, *12*(10), 1815–1822. https://doi.org/10.1111/j.1365-2486.2006.01232.x

Donoghue, D. N. M., Watt, P. J., Cox, N. J., & Wilson, J. (2007). Remote sensing of species mixtures in conifer plantations using LiDAR height and intensity data. *Remote Sensing of Environment*, *110*(4), 509–522. https://doi.org/10.1016/j.rse.2007.02.032

Famiglietti, J. S., Rudnicki, J. W., & Rodell, M. (1998). Variability in surface moisture content along a hillslope transect: Rattlesnake Hill, Texas. *Journal of Hydrology*, *210*(1–4), 259–281. https://doi.org/10.1016/S0022-1694(98)00187-5

Gibson, C. W. D., & Brown, V. K. (1985). Plant succession: theory and applications. *Progress in Physical Geography*, *9*(4), 473–493. https://doi.org/10.1177/030913338500900401

Horn, H. S. (1974). The Ecology of Secondary Succession. *Annual Review of Ecology and Systematics*, *5*(1), 25–37. https://doi.org/10.1146/annurev.es.05.110174.000325(IPCC)

Intergovernmental Panel on Climate Change. (2007). Climate Change 2007: The Physical Science Basis. Summary for Policymakers. New York: Cambridge University Press. Retrieved from www.ipcc.ch/ipccreports/ ar4-wg1.htm

Loughridge, R. (2014). Identifying Topographic Controls of Terrestrial Vegetation Using Remote Sensing Data in a Semiarid Mountain Watershed, Idaho, USA. *Boise State University Theses and Dissertations*. Retrieved from http://scholarworks.boisestate.edu/td/888

Pastor, J., & Post, W. M. (1986). Influence of climate, soil moisture, and succession on forest carbon and nitrogen cycles. *Biogeochemistry*, *2*(1), 3–27. https://doi.org/10.1007/BF02186962